carefully studied, indicate the behavior of the entire structure. The maximum stress may occur at a different location for each individual load.

The individual load cases analyzed are listed in Table 2.10.1-1A. Linear elastic analyses were performed for all load cases except the end impact cases. The normal one foot bottom drop case was analyzed assuming actual plastic behavior of the lead but elastic shell behavior. The 30 foot bottom and lid end drop cases were analyzed inelastically considering the plastic behavior of both lead and shells as described above in the model description. A summary of the stress-strain properties used for each of the individual load cases is given in Table 2.10.1-1B. The meridional and hoop membrane and bending stress components for each of the sixteen ANSYS finite element model load cases are reported in Tables 2.10.1-1 to 2.10.1-15 as listed in Table 2.10.1-1A. These stress components are combined for the various load combinations as described in Sections 2.6 and 2.7 by factoring and algebraic addition. Then the stress intensities of each category are determined and compared to the specified limits. See Sections 2.6 and 2.7. 4

The local stresses at the trunnion locations for cases where the cask is supported on the trunnions are not included in these results. The local stresses are obtained as described below in Section 2.10.1.3 and they are reported in that section. The method used is the "Bijlaard" analysis using hand calculations rather than the ANSYS model.

It should be noted that, for the axisymmetric analyses, the stress is constant around the cask at every location. For asymmetric analyses with significant differences in stress magnitudes on the extreme opposite sides of the cask the stresses at locations on both sides of the cask (contacting side and side opposite contact during impact) are reported. In those cases where the cask is supported on the trunnions, the stresses under transverse loadings (such as gravity) are nearly equal in magnitude on the top and bottom. Therefore only the tensile results for the bottom side are listed for these cases.

The stresses in the portion of the cask body that form the containment boundary are listed in the upper part of each table, locations 1 through 12. All of the locations shown are in the relatively thin portions of the package modeled with the shell elements. The stresses in the flange region modeled with solid elements are much lower than the stresses in the shell and therefore flange stresses are not reported. It should be noted that thin shell theory assumes that the bending stress distribution through the thickness of a thin shell member is linear. Therefore, the bending stress components in a given direction are equal and opposite on the inner and outer surfaces of the shell. The stress components listed in the tables for each location are the membrane stresses in the hoop and meridional directions and the bending stresses in the hoop and meridional directions. The membrane plus bending stress components at the inner and outer surfaces are equal to the membrane stress components $\pm$ the bending stress components.

Note that each table (2.10.1-1 to 2.10.1-15) lists only the stress components at each location for a single load case (except for the end drop cases). These stress components are algebraically added for the various load combinations and the stress intensities are determined, classified and compared with the design criteria of Section 2.1.2 in Sections 2.6 and 2.7. There are no specific limits for individual stress components.

TABLE 2.10.1-1A

INDIVIDUAL LOAD CASES FOR TN-RAM CASK BODY ANALYSIS

LOAD CASE NUMBER	INDIVIDUAL LOAD DESCRIPTION	STRESS RESULT TABLES
1	BOLT PRELOAD	2.10.1-1
2	THERMAL STRESSES AT HOT ENVIRONMENT CONDITION	2.10.1-2
3	THERMAL STRESSES AT COLD ENVIRONMENT CONDITION (-20°F)	2.10.1-3
4	THERMAL STRESSES AT COLD ENVIRONMENT CONDITION (-40°F)	2.10.1-4
5	INTERNAL PRESSURE (P = 30 PSIG)	2.10.1-5
6	EXTERNAL PRESSURE (P = 14.7 PSI)	2.10.1-6
7	GRAVITY (1G DOWN)	2.10.1-7
8	VIBRATION (0.3G LONG., 0.3G HORIZ., 0.6G VERT.)	2.10.1-8
9	SHOCK (2.3G LONG., 1.6G HORIZ., 3.5G VERT.)	2.10.1-9
10	TIE DOWN (10G LONG., 5G HORIZ., 2G VERT.)	2.10.1-10
11	30 FT BOTTOM END DROP - 70G	2.10.1-11
11A	1 FT BOTTOM END DROP - 30G	2.10.1-11A
12	30 FT LID END DROP - 70G	2.10.1-12
13	30 FT SIDE DROP - 128.5 G	2.10.1-12 (CONTACT SIDE) 2.10.1-13A (SIDE OPP. CONTACT)
14	30 FT C.G. OVER CORNER DROP - 68.5G	2.10.1-14 (CONTACT SIDE) 2.10.1-14A (SIDE OPP. CONTACT)
15	THERMAL ACCIDENT	2.10.1-15 (t = 0.56 HRS) 2.10.1-15A (t = 0.83 HRS)

3

TABLE 2.10.1-1B
SUMMARY OF STRESS VS. STRAIN PROPERTIES FOR INDIVIDUAL LOAD CASES

INDIVIDUAL LOAD DESCRIPTION	MATERIAL PROPERTIES USED IN ANALYSIS, E (PSI)		REMARK
	LEAD	304 S.S.	
BOLT PRELOAD	27750	28.3×10^6	
THERMAL STRESS AT HOT ENVIRONMENT CONDITION	27750	28.3×10^6	
THERMAL STRESS (-20°F)	27750	28.3×10^6	
THERMAL STRESS (-40°F)	27750	28.3×10^6	
INTERNAL PRESSURE (30 PSIG)	27750	28.3×10^6	
EXTERNAL PRESSURE (-14.7 PSI)	27750	28.3×10^6	
GRAVITY (1G DOWN)	27750	28.3×10^6	
VIBRATION	27750	28.3×10^6	
SHOCK	27750	28.3×10^6	
TIEDOWN	27750	28.3×10^6	
30 FT BOTTOM END DROP (70G)	PLASTIC LEAD FIG. 2.10.1-1B	PLASTIC S.S. FIG. 2.10.1-1C	
1 FT BOTTOM END DROP (30G)	PLASTIC LEAD FIG. 2.10.1-1B	28.3×10^6	
30 FT LID END DROP (70G)	PLASTIC LEAD FIG. 2.10.1-1B	PLASTIC S.S. FIG. 2.10.1-1C	
30 FT SIDE DROP (128.5G)	27750	28.3×10^6	
30 FT C.G. OVER CORNER DROP (68.5G)	27750	28.3×10^6	
THERMAL ACCIDENT	27750	28.3×10^6	

TABLE 2.10.1-1

CASK BODY STRESSES UNDER BOLT PRELOAD

LOCATION		MEMBRANE STRESSES (PSI)		BENDING STRESSES (PSI)	
		MERIDIONAL SM	HOOP SH	MERIDIONAL SBM	HOOP SBH
	1	28	28	-30	-30
C	2	29	28	-38	-32
O	3	10	46	-23	-4
N	4	0	43	-40	-12
T	5	0	-1	-1	-0
A	6	0	0	0	0
I	7	0	0	-0	-0
N	8	0	0	0	0
M	9	0	0	0	0
E	10	1	-0	4	1
N	11	0	-0	4	1
T	12	0	0	0	0
	13	-1	-1	-7	-7
C	14	-1	-1	26	7
O	15	-1	-1	25	8
N	16	-0	19	-45	-13
T	17	-0	20	2	1
N A	18	-0	-1	1	0
O I	19	-0	0	-0	-0
N N	20	-0	-0	-0	-0
M	21	-0	-0	0	0
E	22	-0	-0	-0	-0
N	23	-0	-0	-2	-1
T	24	-0	-0	-1	0
	25	-0	-0	1	1

3

TABLE 2.10.1-2

CASK BODY STRESSES UNDER HOT ENVIRONMENT CONDITION

LOCATION		MEMBRANE STRESSES (PSI)		BENDING STRESSES (PSI)	
		MERIDIONAL SM	HOOP SH	MERIDIONAL SBM	HOOP SBH
	1	280	280	-558	-556
C	2	258	273	-352	-497
O	3	990	-1,345	-2,697	304
N	4	-218	-1,657	2,353	706
T	5	-236	-1,965	-49	-15
A	6	-235	-1,914	17	5
I	7	-235	-1,939	0	0
N	8	-235	-1,938	-1	-0
M	9	-235	-1,922	-39	-12
E	10	-450	-323	-6,442	-1,924
N	11	-774	-420	-6,442	-1,857
T	12	-777	-777	-183	-248
	13	388	388	-301	-329
C	14	388	388	-5,955	-1,516
O	15	432	401	-5,804	-1,741
N	16	403	317	-1,921	-576
T	17	434	261	3,555	1,066
N A	18	395	1,353	-297	-89
O I	19	399	1,336	24	7
N N	20	399	1,340	0	0
M	21	399	1,342	-2	-1
E	22	399	1,293	155	47
N	23	454	275	4,467	1,340
T	24	199	199	1,645	16
	25	199	199	-1,192	-1,188

3

TABLE 2.10.1-3

CASK BODY STRESSES UNDER -20°F UNIFORM TEMPERATURE

LOCATION		MEMBRANE STRESSES (PSI)		BENDING STRESSES (PSI)	
		MERIDIONAL SM	HOOP SH	MERIDIONAL SBM	HOOP SBH
	1	1	1	5	9
C	2	1	1	-5	-2
O	3	5	-8	-38	-5
N	4	-1	-24	-84	-25
T	5	-0	-119	-2	-1
A	6	0	-116	2	0
I	7	0	-116	0	0
N	8	0	-116	-0	-0
M	9	0	-103	13	4
E	10	-21	-67	-1,711	-504
N	11	-326	-159	-1,766	-448
T	12	-335	-335	613	609
	13	-5	-4	-152	-232
C	14	-3	-3	98	24
O	15	-2	-3	90	27
N	16	-1	0	-12	-4
T	17	0	-5	11	3
N A	18	-0	0	-1	-0
O I	19	0	0	0	0
N N	20	-0	0	0	0
M	21	-0	0	0	0
E	22	-0	-0	-0	-0
N	23	-0	-0	-0	-0
T	24	-0	-0	-0	0
	25	-0	-0	0	0

3

TABLE 2.10.1-4

CASK BODY STRESSES UNDER -40°F UNIFORM TEMPERATURE

LOCATION		MEMBRANE STRESSES (PSI)		BENDING STRESSES (PSI)	
		MERIDIONAL SM	HOOP SH	MERIDIONAL SBM	HOOP SBH
	1	1	1	7	11
C	2	1	1	-7	-2
O	3	6	-9	-46	-6
N	4	-1	-29	-103	-31
T	5	-0	-146	-3	-1
A	6	0	-142	2	1
I	7	0	-142	0	0
N	8	0	-142	-0	-0
M	9	0	-126	15	5
E	10	-26	-82	-2,091	-616
N	11	-398	-194	-2,159	-547
T	12	-409	-409	749	745
	13	-6	-5	-185	-284
C	14	-4	-4	119	29
O	15	-2	-3	110	33
N	16	-1	0	-15	-4
T	17	0	-6	14	4
N A	18	-0	0	-1	-0
O I	19	0	0	0	0
N N	20	-0	0	0	0
M	21	-0	0	0	0
E	22	-0	-0	-0	-0
N	23	-0	-0	-0	-0
T	24	-0	-0	-0	0
	25	-0	-0	0	0

3

TABLE 2.10.1-5

CASK BODY STRESSES UNDER 30 PSIG INTERNAL PRESSURE

LOCATION		MEMBRANE STRESSES (PSI)		BENDING STRESSES (PSI)	
		MERIDIONAL SM	HOOP SH	MERIDIONAL SBM	HOOP SBH
	1	64	64	-1,420	-1,502
C	2	41	57	878	-33
O	3	-28	-70	740	107
N	4	179	185	-365	-105
T	5	182	644	17	10
A	6	182	645	7	7
I	7	182	644	6	6
N	8	182	644	6	6
M	9	182	656	41	17
E	10	324	-37	4,205	1,247
N	11	307	-42	4,345	1,139
T	12	327	327	28	-29
	13	-47	-47	166	75
C	14	-47	-47	2,239	506
O	15	-152	-74	2,116	635
N	16	-104	13	-1,842	-552
T	17	63	-58	203	61
N A	18	61	29	-18	-5
O I	19	61	26	2	0
N N	20	61	26	0	0
M	21	61	26	0	0
E	22	61	35	-6	-2
N	23	81	63	1,642	493
T	24	56	56	606	-65
	25	56	56	-1,425	-1,443

3

TABLE 2.10.1-6

CASK BODY STRESSES UNDER 14.7 PSIG EXTERNAL PRESSURE

LOCATION		MEMBRANE STRESSES (PSI)		BENDING STRESSES (PSI)	
		MERIDIONAL SM	HOOP SH	MERIDIONAL SBM	HOOP SBH
	1	-63	-63	452	376
C	2	-63	-63	-372	17
O	3	-7	2	-140	-24
N	4	-60	-41	221	66
T	5	-61	-24	1	0
A	6	-61	-24	0	0
I	7	-61	-24	-0	-0
N	8	-61	-24	-0	-0
M	9	-62	-28	-9	-3
E	10	-108	51	-1,160	-341
N	11	-42	70	-1,231	-308
T	12	-48	-48	219	210
	13	12	12	99	99
C	14	12	12	-227	-57
O	15	10	11	-220	-66
N	16	2	-45	390	117
T	17	-103	-29	-329	-101
N A	18	-100	-229	28	6
O I	19	-100	-223	-6	-4
N N	20	-100	-222	-3	-3
M	21	-100	-222	-3	-3
E	22	-100	-232	-4	-4
N	23	-118	-78	-1,528	-460
T	24	-60	-60	-566	20
	25	-60	-60	859	869

3

TABLE 2.10.1-7

CASK BODY STRESSES UNDER 1G VERTICAL LOAD

LOCATION		MEMBRANE STRESSES (PSI)		BENDING STRESSES (PSI)	
		MERIDIONAL SM	HOOP SH	MERIDIONAL SBM	HOOP SBH
	1	24	-1	-4	-10
C	2	-4	26	12	-8
O	3	-8	-9	-15	4
N	4	-9	-34	147	41
T	5	10	2	-6	-23
A	6	28	9	-12	-38
I	7	54	22	-21	-56
N	8	53	8	-18	-47
M	9	51	-2	-5	-26
E	10	68	61	153	44
N	11	46	55	184	43
T	12	17	12	-24	-10
	13	8	18	-6	-5
C	14	42	111	-544	-139
O	15	45	112	-575	-172
N	16	29	36	-236	-71
T	17	4	28	79	20
N A	18	-40	161	29	-9
O I	19	46	105	-19	-34
N N	20	136	104	-30	-51
M	21	68	112	-27	-42
E	22	-47	166	49	-6
N	23	2	34	93	28
T	24	5	35	30	7
	25	28	6	1	-11

3

TABLE 2.10.1-8

CASK BODY STRESSES UNDER VIBRATION LOAD

LOCATION		MEMBRANE STRESSES (PSI)		BENDING STRESSES (PSI)	
		MERIDIONAL SM	HOOP SH	MERIDIONAL SBM	HOOP SBH
	1	49	32	-260	-302
C	2	29	50	140	-13
O	3	-28	-72	-202	-10
N	4	-85	-176	537	159
T	5	-74	-89	-7	-16
A	6	-61	-65	-5	-24
I	7	-41	-10	-12	-37
N	8	-39	27	-11	-31
M	9	-40	46	-8	-19
E	10	-69	40	-226	-66
N	11	23	69	-230	-51
T	12	2	-2	125	140
	13	6	12	-51	-59
C	14	29	75	-315	-83
O	15	32	76	-346	-104
N	16	24	48	-340	-102
T	17	85	6	232	67
N A	18	56	174	2	-11
O I	19	115	120	-12	-23
N N	20	179	87	-21	-34
M	21	136	60	-19	-28
E	22	-40	58	26	-6
N	23	-6	21	-32	-9
T	24	4	24	-14	8
	25	19	4	52	45

3

TABLE 2.10.1-9

CASK BODY STRESSES UNDER SHOCK LOAD

LOCATION		MEMBRANE STRESSES (PSI)		BENDING STRESSES (PSI)	
		MERIDIONAL SM	HOOP SH	MERIDIONAL SBM	HOOP SBH
	1	343	249	-1,986	-2,306
C	2	231	349	1,059	-90
O	3	-203	-538	-1,532	-81
N	4	-637	-1,304	3,927	1,166
T	5	-582	-681	-42	-95
A	6	-501	-507	-26	-139
I	7	-385	-108	-67	-213
N	8	-368	193	-59	-178
M	9	-369	352	-54	-112
E	10	-617	231	-1,933	-565
N	11	119	454	-2,000	-447
T	12	-7	-27	988	1,085
	13	33	70	-382	-444
C	14	165	431	-1,717	-458
O	15	188	438	-1,912	-573
N	16	148	324	-2,307	-692
T	17	646	9	1,680	489
N A	18	481	1,123	-21	-74
O I	19	825	783	-66	-129
N N	20	1,196	533	-120	-197
M	21	954	315	-110	-163
E	22	-244	231	139	-37
N	23	-48	116	-361	-108
T	24	23	137	-144	49
	25	109	26	399	358

TABLE 2.10.1-10

CASK BODY STRESSES UNDER TIE-DOWN LOAD

LOCATION			MEMBRANE STRESSES (PSI)		BENDING STRESSES (PSI)	
			MERIDIONAL SM	HOOP SH	MERIDIONAL SBM	HOOP SBH
		1	1,222	1,091	-8,593	-9,914
	C	2	1,052	1,226	4,464	-303
	O	3	-791	-2,232	-6,492	-397
	N	4	-2,672	-5,283	15,403	4,604
	T	5	-2,642	-2,980	-109	-147
	A	6	-2,502	-2,311	19	-177
	I	7	-2,285	-724	-58	-287
	N	8	-2,208	748	-46	-237
	M	9	-2,181	1,555	-180	-187
	E	10	-3,451	309	-10,142	-2,956
	N	11	-8	1,344	-10,781	-2,431
	T	12	-223	-250	4,566	4,836
		13	50	102	-1,587	-1,872
	C	14	240	616	-1,291	-418
	O	15	308	636	-1,784	-534
	N	16	314	1,005	-7,351	-2,206
	T	17	2,763	-283	6,408	1,901
N	A	18	2,541	3,049	-421	-221
O	I	19	3,070	2,204	-68	-173
N	N	20	3,649	1,132	-176	-278
	M	21	3,373	90	-172	-233
	E	22	-523	-878	51	-94
	N	23	-229	117	-2,626	-787
	T	24	41	200	-973	131
		25	161	45	1,728	1,681

3

TABLE 2.10.1-11

CASK BODY STRESSES UNDER 30 FOOT BOTTOM END DROP - 70G

LOCATION		MEMBRANE STRESS COMPONENTS (PSI)		STRESS INTENSITIES (PSI)		
				MEMBRANE	MEMBRANE + BENDING	
		MERIDIONAL	HOOP	AVERAGE	INNER SURFACE	OUTER SURFACE
	1	-997	-997	1,052	7,371	9,476
C	2	-615	-865	920	7,782	7,247
O	3	195	2,193	2,193	6,643	5,370
N	4	-2,956	-124	2,956	4,306	10,218
T	5	-3,263	37	3,300	3,322	3,279
A	6	-3,516	-0	3,516	3,517	3,516
I	7	-4,075	-6	4,075	4,070	4,080
N	8	-4,634	-8,079	8,079	8,103	8,056
M	9	-4,915	-17,383	17,383	16,960	19,308
E	10	-23,863	17,658	41,521	44,229	41,593
N	11	-30,523	-703	30,185	42,245	39,373
T	12	-19,265	-19,355	19,016	31,132	32,739
	13	3,272	3,272	3,272	5,973	705
C	14	3,272	3,272	3,272	4,085	4,476
O	15	3,597	100	3,597	2,893	10,086
N	16	3,630	1,709	3,630	7,068	677
T	17	-1,863	1,700	3,563	2,970	6,527
N A	18	-6,149	-609	6,149	4,312	7,986
O I	19	-6,609	-1,022	6,609	6,154	7,063
N N	20	-7,250	54	7,304	7,252	7,356
M	21	-7,854	2,599	10,453	8,150	12,756
E	22	-9,372	10,332	19,704	13,673	22,138
N	23	-24,663	12,228	36,891	43,796	42,162
T	24	-3,079	-4,927	6,260	36,610	36,483
	25	-8,181	-8,207	9,540	39,581	40,771

TABLE 2.10.1-11A

CASK BODY STRESSES UNDER 1 FT BOTTOM END DROP - 30G

LOCATION		MEMBRANE STRESS COMPONENTS (PSI)		STRESS INTENSITIES (PSI)		
				MEMBRANE Pm or (P1)*	MEMBRANE + BENDING Pm + Pb or (P1 + Pb + Q)*	
		MERIDIONAL	HOOP	AVERAGE	INNER SURFACE	OUTER SURFACE
	1	-392	-392	415	3,132	3,962
C	2	-178	-318	341	3,325	3,149
O	3	-162	601	763	2,274	1,454
N	4	-1,326	-75	1,326	2,268	4,920
T	5	-1,461	-12	1,461	1,440	1,482
A	6	-1,570	0	1,570	1,570	1,570
I	7	-1,809	0	1,810	1,810	1,809
N	8	-2,048	-447	2,048	1,954	2,142
M	9	-2,186	-719	2,186	1,847	2,526
E	10	-4,154	13,532	17,685	47,775	38,616
N	11	-4,417	176	4,593	34,126	25,583
T	12	-3,994	-4,023	3,878	1,984	9,681
	13	1,172	1,172	1,172	1,812	575
C	14	1,172	1,172	1,172	1,416	1,264
O	15	1,536	357	1,536	126	3,147
N	16	1,557	757	1,557	2,841	371
T	17	-800	360	1,160	1,588	732
N A	18	-2,294	34	2,328	2,505	2,181
O I	19	-2,482	-273	2,482	2,409	2,556
N N	20	-2,756	192	2,949	2,948	2,950
M	21	-3,025	-22	3,025	2,688	3,474
E	22	-3,685	1,617	5,302	4,287	6,318
N	23	-4,187	7,502	11,689	33,900	25,525
T	24	-1,218	-1,218	1,789	17,172	17,172
	25	-1,218	-1,218	1,789	32,810	36,389

TABLE 2.10.1-12

CASK BODY STRESSES UNDER 30 FOOT LID END DROP - 70G

LOCATION		MEMBRANE STRESS COMPONENTS (PSI)		STRESS INTENSITIES (PSI)		
				MEMBRANE	MEMBRANE + BENDING	
		MERIDIONAL	HOOP	AVERAGE	INNER SURFACE	OUTER SURFACE
	1	-11,621	-11,624	12,886	36,852	38,029
C	2	-8,724	-7,803	9,986	41,231	39,180
O	3	1,378	12,873	12,873	23,429	20,986
N	4	-5,823	5,079	10,902	7,098	14,631
T	5	-5,591	-7,572	7,572	7,336	7,807
A	6	-5,345	-7,336	7,336	7,421	7,251
I	7	-4,785	-5	4,785	4,780	4,789
N	8	-4,226	-3	4,226	4,223	4,230
M	9	-3,897	-1,069	3,897	3,588	4,207
E	10	-13,338	14,495	27,834	35,201	33,620
N	11	-6,028	72	6,100	23,522	18,086
T	12	-5,079	-5,116	5,116	4,325	5,956
	13	15,520	15,659	15,973	31,693	26,596
C	14	20,931	14,613	20,931	33,409	36,629
O	15	11,082	9,148	11,082	25,831	33,914
N	16	9,627	28,865	28,865	33,322	32,828
T	17	-13,546	7,414	20,960	24,596	14,549
N A	18	-10,478	6,587	17,065	16,200	17,931
O I	19	-7,682	6,213	13,895	14,170	13,621
N N	20	-7,040	62	7,102	7,057	7,146
M	21	-6,400	-956	6,400	6,031	6,770
E	22	-5,879	-618	5,879	6,391	5,367
N	23	-1,558	2,088	3,646	14,636	11,521
T	24	-491	-491	549	7,374	7,374
	25	-491	-491	549	11,241	12,338

3

TABLE 2.10.1-13

CASK BODY STRESSES UNDER 30 FOOT SIDE DROP (128.5 G) - CONTACT SIDE

LOCATION		MEMBRANE STRESSES (PSI)		BENDING STRESSES (PSI)	
		MERIDIONAL SM	HOOP SH	MERIDIONAL SBM	HOOP SBH
	1	-20,516	-2,937	-260	-2,169
C	2	-23,417	-22,753	-936	-1,455
O	3	-4,335	-19,324	9,832	1,183
N	4	343	-14,789	28,491	9,533
T	5	10,908	9,255	-852	-907
A	6	16,866	7,748	-1,472	-2,187
I	7	18,891	6,557	-1,686	-3,004
N	8	8,987	3,234	-878	-1,509
M	9	1,423	-882	-1,557	-647
E	10	-2,332	-7,141	-16,824	-5,007
N	11	-5,691	-8,087	-9,897	-3,629
T	12	-2,344	-472	-2,768	-3,660
	13	581	2,961	-967	-833
C	14	5,046	19,259	-65,985	-16,140
O	15	5,650	19,440	-71,517	-21,475
N	16	1,620	-15,242	-55,923	-17,108
T	17	5,909	-22,889	54,083	17,131
N A	18	18,385	12,310	-8,166	-2,739
O I	19	28,443	11,097	-1,647	-1,471
N N	20	39,279	11,657	-3,066	-2,407
M	21	31,096	13,035	-1,786	-593
E	22	16,312	20,851	-14,592	-3,068
N	23	-1,050	-10,776	-122,330	-37,907
T	24	-17,443	-17,597	-57,379	-38,019
	25	-14,968	-2,193	-12,194	-15,883

TABLE 2.10.1-13A

CASK BODY STRESSES UNDER 30 FOOT SIDE DROP
(128.5G) - SIDE OPPOSITE CONTACT

LOCATION		MEMBRANE STRESSES (PSI)		BENDING STRESSES (PSI)	
		MERIDIONAL SM	HOOP SH	MERIDIONAL SBM	HOOP SBH
	1	-9,150	1,600	-654	-2,395
C	2	-8,095	8,955	-6,777	-3,541
O	3	505	2,823	320	2,484
N	4	-1,024	3,716	10,495	4,075
T	5	-4,782	-776	-268	-791
A	6	-7,940	-937	-493	-1,952
I	7	-10,611	-692	-542	-2,719
N	8	-5,196	2,196	-48	-1,319
M	9	-161	5,827	677	-35
E	10	6,789	8,635	57,422	16,688
N	11	2,178	7,254	58,407	14,160
T	12	-970	3,414	-2,305	-3,392
	13	-1,071	-2,287	473	-6
C	14	-5,537	-15,206	71,831	18,196
O	15	-5,825	-15,292	75,867	22,740
N	16	-3,876	10,221	37,002	10,770
T	17	-8,960	-952	-14,546	-3,457
N A	18	-19,095	-10,970	4,253	987
O I	19	-25,972	-9,695	479	-833
N N	20	-34,022	-9,954	881	-1,223
M	21	-30,877	-11,091	1,439	374
E	22	-23,651	-13,965	1,883	1,875
N	23	-4,463	16,557	-58,796	-17,058
T	24	-4,676	16,437	-23,058	-10,622
	25	-7,151	2,514	-2,230	-10,146

TABLE 2.10.1-14

CASK BODY STRESSES UNDER 30 FOOT C.G OVER CORNER DROP (68.54G) - CONTACT SIDE

LOCATION			MEMBRANE STRESSES (PSI)		BENDING STRESSES (PSI)	
			MERIDIONAL SM	HOOP SH	MERIDIONAL SBM	HOOP SBH
		1	-7,477	-1,854	31,036	39,338
	C	2	-9,666	-14,117	-12,255	15,869
	O	3	521	17,516	-62,540	-11,743
	N	4	-24,173	6,182	68,091	21,901
	T	5	-23,500	-50	-3,932	3,080
	A	6	-22,818	-9,884	2,309	6,814
	I	7	-19,501	884	3,831	9,463
	N	8	-14,429	11,936	4,929	7,929
	M	9	-10,868	-836	5,078	5,171
	E	10	-10,500	2,963	3,200	1,135
	N	11	-1,681	5,617	3,932	1,575
	T	12	-2,428	1,077	29,413	31,470
		13	-1,116	2,395	17,689	14,948
	C	14	-31	14,924	14,934	4,234
	O	15	69	14,954	4,881	1,358
	N	16	-6,811	-15,225	26,258	7,762
	T	17	-40,018	-571	-23,332	-5,541
N	A	18	-33,156	5,105	6,816	6,885
O	I	19	-29,950	7,949	2,426	7,884
N	N	20	-22,504	1,153	4,390	10,748
	M	21	-15,270	-5,798	4,364	8,799
	E	22	-6,750	-2,046	1,634	5,271
	N	23	-1,803	1,254	-29,899	-8,881
	T	24	-800	1,571	-11,133	573
		25	-214	593	11,259	12,374

3

TABLE 2.10.1-14A

CASK BODY STRESSES UNDER 30 FOOT C.G OVER CORNER DROP (68.54G) - SIDE OPPOSITE CONTACT

LOCATION		MEMBRANE STRESSES (PSI)		BENDING STRESSES (PSI)	
		MERIDIONAL SM	HOOP SH	MERIDIONAL SBM	HOOP SBH
	1	-4,450	603	-9,176	16,166
C	2	-3,269	2,216	-12,359	-4,766
O	3	2,156	7,368	8,423	1,978
N	4	7,201	13,579	-25,031	-6,044
T	5	2,956	-1,981	-3,913	3,078
A	6	-1,731	-10,663	1,904	6,684
I	7	-9,347	-348	3,647	9,400
N	8	-11,840	10,527	4,958	7,930
M	9	-10,917	-2,705	5,148	5,184
E	10	-12,280	682	-7,993	-2,099
N	11	-2,626	3,578	-7,907	-1,408
T	12	-2,610	496	29,919	31,758
	13	-1,481	1,260	9,144	10,029
C	14	-2,395	7,473	57,546	14,835
O	15	-2,714	7,378	48,852	14,549
N	16	-7,187	983	-21,384	-6,531
T	17	552	478	-4,810	15
N A	18	-793	1,642	5,256	6,417
O I	19	-3,870	5,234	1,762	7,685
N N	20	-8,680	-1,516	4,129	10,670
M	21	-9,966	-8,387	4,393	8,808
E	22	-4,647	-4,551	1,603	5,262
N	23	-1,895	-83	-33,712	-10,046
T	24	-1,234	110	-12,532	-233
	25	-2,018	252	11,090	12,277

3

TABLE 2.10.1-15

CASK BODY STRESSES UNDER THERMAL ACCIDENT (TIME = 0.56 HRS)

LOCATION		MEMBRANE STRESSES (PSI)		BENDING STRESSES (PSI)	
		MERIDIONAL SM	HOOP SH	MERIDIONAL SBM	HOOP SBH
	1	3,937	3,937	9,031	9,034
C	2	4,395	4,074	12,775	9,990
O	3	-50	-177	-3,104	-4,954
N	4	-65	-10,982	-9,244	-2,773
T	5	3	9	311	93
A	6	-0	2	-2	-1
I	7	0	-0	0	0
N	8	-0	-2	-15	-4
M	9	-15	420	-4,235	-1,271
E	10	115	-12,815	-77	224
N	11	806	2,840	1,422	2,684
T	12	649	649	3,415	3,415
	13	681	681	2,038	1,977
C	14	681	681	-13,110	-3,368
O	15	755	704	-12,923	-3,877
N	16	278	2,839	23,230	6,969
T	17	517	2,677	7,690	2,307
N A	18	343	442	-9,387	-2,816
O I	19	459	736	1,671	501
N N	20	440	539	5	2
M	21	442	337	478	144
E	22	335	-948	-10,668	-3,200
N	23	621	112	17,766	5,330
T	24	-106	-106	5,964	4,692
	25	-106	-106	3,910	3,910

3

TABLE 2.10.1-15A

CASK BODY STRESSES UNDER THERMAL ACCIDENT (TIME = 0.83 HRS)

LOCATION		MEMBRANE STRESSES (PSI)		BENDING STRESSES (PSI)	
		MERIDIONAL SM	HOOP SH	MERIDIONAL SBM	HOOP SBH
	1	4,165	4,165	8,954	8,958
C	2	4,641	4,308	12,656	9,904
O	3	-942	-3,467	-283	-4,382
N	4	-7	-17,987	-1,227	-368
T	5	-6	299	-829	-249
A	6	1	-80	37	11
I	7	0	0	0	0
N	8	-1	-9	-58	-17
M	9	-17	373	-3,957	-1,187
E	10	215	-19,508	-66	380
N	11	1,424	4,757	2,036	4,296
T	12	1,168	1,168	5,605	5,605
	13	643	643	2,036	1,977
C	14	643	643	-12,526	-3,219
O	15	715	665	-12,354	-3,706
N	16	242	2,988	23,323	6,997
T	17	636	-12	-6,200	-1,860
N A	18	649	1,275	-4,738	-1,421
O I	19	712	960	1,186	356
N N	20	698	913	4	1
M	21	699	728	294	88
E	22	649	665	-5,585	-1,675
N	23	918	338	20,525	6,157
T	24	90	90	6,969	4,798
	25	90	90	3,366	3,366

2.10.1.2 BIJLAARD TRUNNION ANALYSIS

This section discusses the analysis performed to calculate the local stresses in the cask body outer shell at the trunnion locations due to the loadings applied through the trunnions. These local effects are not included in the ANSYS stress results tables reported above in Section 2.10.1.2. The local stresses must be superimposed on the above stress results for the cases where the inertial loadings are reacted at the trunnions. The local stresses are calculated in accordance with the methodology of Reference WRC-107* which is based on the "Bijlaard" analysis for local stresses in cylindrical shells due to external loadings.

Loading

The Bijlaard analysis was performed for several different trunnion loading conditions to support various structural evaluation cases. A summary of the load cases considered is provided in Table 2.10.1-16A.

Section 2.5 of Chapter Two provides the analyses of the trunnions under the limiting 2/5/10 g tiedown loading (cask horizontal) and the 3 g lifting (cask vertical) loading. Those analyses were performed to demonstrate that the trunnions satisfy the performance requirements of 10CFR71.45. The Bijlaard analysis for these two load cases was performed to verify that the trunnion induced stresses in the cask body outer shell are also acceptable.

* Welding Research Council Bulletin No. 107
Local Stresses in Spherical and Cylindrical Shell Due to External Loading, March 1979 Revision

TABLE 2.10.1-16A

LOAD CASES FOR TN-RAM CASK BODY LOCAL STRESS ANALYSIS USING BIJLAARD METHOD

LOAD CASE NUMBER	INDIVIDUAL LOAD DESCRIPTION	STRESS RESULT TABLES
16	LOCAL STRESSES AT TRUNNION / CASK BODY INTERFACE - CASK HORIZONTAL W/ 1G VERTICAL LOADING	2.10.1-16
17	LOCAL STRESSES AT TRUNNION / CASK BODY INTERFACE - WITH VIBRATION LOADING	2.10.1-17
18	LOCAL STRESSES AT TRUNNION / CASK BODY INTERFACE - WITH SHOCK LOADING	2.10.1-18
19	LOCAL STRESSES AT TRUNNION / CASK BODY INTERFACE - CASK VERTICAL W/ 3G LIFTING LOAD	2.10.1-19
20	LOCAL STRESSES AT TRUNNION / CASK BODY INTERFACE - CASK HORIZONTAL W/ 3G LIFTING LOAD	2.10.1-20
21	LOCAL STRESSES AT TRUNNION / CASK BODY INTERFACE - WITH TIE DOWN LOADING	2.10.1-21
22	STRESSES DUE TO TIE DOWN LOAD INCLUDING LOCAL STRESSES AT TRUNNION/CASK BODY INTERFACE	2.10.1-22
23	STRESSES DUE TO 3G LIFTING LOAD INCLUDING LOCAL STRESSES AT TRUNNION / CASK BODY INTERFACE	2.10.1-23

Three additional load cases were analyzed to support the normal condition of transport load combinations described in Section 2.6 of Chapter Two. A 1g-vertical (cask horizontal) load case is applicable for load combinations as identified in Table 2.6-1A in Section 2.6 of Chapter 2.0. The vibration and shock loading cases pertain to load combinations involving specific transport loadings (see Table 2.6-1A). The shock/vibration inertia values used for vibration and shock conditions were obtained from truck bed accelerations in ANSI N14.23*.

Loads used for the "Bijlaard" analysis are obtained from the packaging inertial loadings and are listed in Table 2.10.1-16B. The loads are based on a transport weight of 80,000 lb. which is larger than the calculated weight of 79,000 lb.

Method of Analysis

The local stresses induced in the outer shell cylinder by the trunnions are calculated using "Bijlaard's" method. The trunnion is approximated by an equivalent attachment so that the curves of the Reference WRC-107 can be used to obtain the necessary coefficients. These resulting coefficients are inserted into blanks in the column entitled "Read Curves For," in a standard computation form, a sample

* Draft American National Standard Design Basis for Resistance to Shock and Vibration, ANSI N14.23, May, 1980.

TABLE 2.10.1-16B

TRUNNION LOADING

LOADING DESCRIPTION	INERTIAL LOAD	MAX. TRUNNION LOAD FRONT TRUNNION	REAR TRUNNION
GRAVITY (Cask Horizontal)	1 G (Vertical)	V_c = 20 KIPS M_c = 48.8 IN-KIPS	V_c = 20 KIPS M_c = 32.4 IN-KIPS
LIFTING (Cask Vertical)	3 G (Longitudinal)	V_L = 120 KIPS M_L = 644.4 IN-KIPS	V_L = 0 M_L = 0
LIFTING (Cask Horizontal)	3 G (Vertical)	V_L = 60 KIPS M_L = 322.2 IN-KIPS	V_L = 60 KIPS M_L = 296.4 IN-KIPS
SHOCK (Cask Horizontal)	2.3 G (Longitudinal)	V_L = 0 V_c = 70 KIPS	V_L = 92 KIPS V_c = 70 KIPS
	1.6 G (Lateral)	P = 64 KIPS M_L = 0	P = 64 KIPS M_L = 149 IN-KIPS
	0.6 G (Lateral)	M_c = 170.8 IN-KIPS	M_c = 113.4 IN-KIPS
VIBRATION (Cask Horizontal)	0.3 G (Longitudinal)	V_L = 0 V_c = 12 KIPS	V_L = 12 KIPS V_c = 12 KIPS
	0.3 G (Lateral)	P = 12 KIPS M_L = 0	P = 12 KIPS M_L = 19.4 IN-KIPS
	0.6 G (Lateral)	M_c = 29.3 IN-KIPS	M_c = 19.4 IN-KIPS
TIE-DOWN (Cask Horizontal)	10 G (Longitudinal)	V_L = 0 V_c = 40 KIPS	V_L = 400 KIPS V_c = 40 KIPS
	1.6 G (Lateral)	P = 200 KIPS M_L = 0	P = 200 KIPS M_L = 64.8 IN-KIPS
	0.6 G (Lateral)	M_c = 97.6 IN-KIPS	M_c = 64.8 IN-KIPS

of which is attached as Table 2.10.1-16C. The stresses are calculated by performing the indicated multiplication in the column entitled "Compute Absolute Values of Stress and Enter Result". The resulting stress is inserted into the stress table at the eight stress locations, i.e., AU, AL, BU, BL, etc. Note that the sign convention for this table is defined on the figure as if the load directions are as shown. The membrane plus bending stresses are calculated by completing Table 2.10.1-16C.

Model, Boundary Conditions and Assumptions

The cylindrical body is assumed to be a hollow cylinder of infinite length. Since the trunnions are located away from the ends of the cylinder, this assumption is acceptable because the local effects are not significantly affected by the end restraints, i.e., lid and bottom. This is conservative since end restraints would reduce the local bending effects.

Results of Analysis

The attachment parameter, β, is obtained by using an attachment radius, r_o, equal to the radius of the trunnion base plate. For the "Bijlaard" parameter computations, an equivalent cylinder thickness is employed. The equivalent thickness has the same bending stiffness as the layered wall consisting of the outer shell, lead and inner shell. The equivalent thickness is determined assuming the layers can slide relative to each other (unbonded lead).

TABLE 2.10.1-16C

BIJLAARD COMPUTATION SHEET

1 APPLIED LOADS

RADIAL LOAD P = _____ LB

CIRC. MOMENT M_c = _____ IN-LB

LONG. MOMENT M_L = _____ IN-LB

TORSION MOMENT M_T = _____ IN-LB

SHEAR LOAD V_c = _____ LB

SHEAR LOAD V_L = _____ LB

* NOTE: ENTER ALL FORCE VALUES IN ACCORDANCE WITH SIGN CONVENTION

2 GEOMETRY

VESSEL THICKNESS T = _____ IN

ATTACHMENT RADIUS r_o = _____ IN

VESSEL RADIUS R_m = _____ IN

3 GEOMETRIC PARAMETERS

$\gamma = \frac{R_m}{T} =$ _____

$\beta = 10.0731 \frac{r_o}{\sqrt{R_m T}} =$ _____

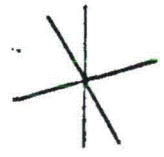

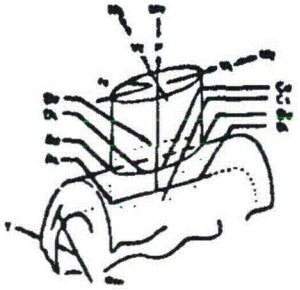

FROM PG	READ CURVES FOR	COMPUTE ABSOLUTE VALUES OF STRESS AND ENTER RESULT	STRESSES - IF LOAD IS OPPOSITE THAT SHOWN, REVERSE SIGNS SHOWN							
			A_0	A_1	B_0	B_1	C_0	C_1	D_0	D_1
2C AND 4C	$\frac{M_c}{P/R_m}$ *	$\left(\frac{M_c}{P/R_m}\right)\frac{P}{T^2}$ *	+	+	+	+	+	+	+	+
2C AND 2C-1	$\frac{M_L}{P}$ *	$\left(\frac{M_L}{P}\right)\frac{P}{T^2}$ *	+	−	+	−	+	−	+	−
2A	$\frac{M_c}{M_c/R_m\beta}$ *	$\left(\frac{M_c}{M_c/R_m\beta}\right)\frac{M_c\beta}{T^2}$ *					−	−	+	+
4A	$\frac{M_c}{M_c/R_m\beta}$ *	$\left(\frac{M_c}{M_c/R_m\beta}\right)\frac{M_c\beta}{T^2}$ *					−	+	+	−
2B	$\frac{M_c}{M_L/R_m\beta}$ *	$\left(\frac{M_c}{M_L/R_m\beta}\right)\frac{M_L\beta}{T^2}$ *	−	−	+	+				
4B OR 4B-1	$\frac{M_c}{M_L/R_m\beta}$ *	$\left(\frac{M_c}{M_L/R_m\beta}\right)\frac{M_L\beta}{T^2}$ *	−	+	+	−				
ADD ALGEBRAICALLY FOR SUMMATION OF σ_x STRESSES σ_x *										
3C AND 4C	$\frac{M_T}{P/R_m}$ *	$\left(\frac{M_T}{P/R_m}\right)\frac{P}{T^2}$ *	+	+	+	+	+	+	+	+
3C-1 AND 3C	$\frac{M_T}{P}$ *	$\left(\frac{M_T}{P}\right)\frac{P}{T^2}$ *	+	−	+	−	+	−	+	−
4A	$\frac{M_T}{M_c/R_m\beta}$ *	$\left(\frac{M_T}{M_c/R_m\beta}\right)\frac{M_c\beta}{T^2}$ *					−	−	+	+
3A	$\frac{M_T}{M_c/R_m\beta}$ *	$\left(\frac{M_T}{M_c/R_m\beta}\right)\frac{M_c\beta}{T^2}$ *					−	+	+	−
4B	$\frac{M_T}{M_L/R_m\beta}$ *	$\left(\frac{M_T}{M_L/R_m\beta}\right)\frac{M_L\beta}{T^2}$ *	−	−	+	+				
3B OR 3B-1	$\frac{M_T}{M_L/R_m\beta}$ *	$\left(\frac{M_T}{M_L/R_m\beta}\right)\frac{M_L\beta}{T^2}$ *	−	+	+	−				
ADD ALGEBRAICALLY FOR SUMMATION OF σ_θ STRESSES σ_θ *										
SHEAR STRESS DUE TO TORSION M_T	$\tau_{x\theta} = \tau_{\theta x} = \frac{M_T}{T^2}$		+	+	+	+	+	+	+	+
SHEAR STRESS DUE TO LOAD V_c	$\tau_{x\theta} = \frac{V_c}{T^2}$		+	+	−	−				
SHEAR STRESS DUE TO LOAD V_L	$\tau_{\theta x} = \frac{V_L}{T^2}$						+	+	−	−
ADD ALGEBRAICALLY FOR SUMMATION OF SHEAR STRESSES τ *										

LONGITUDINAL σ_x

PRESSURE STRESS $\frac{PR_m}{2T}$ * = _____ *

LONGITUDINAL BENDING STRESS = _____ *

TOTAL MEMBRANE STRESS = _____ * = _____ ksi

TOTAL BENDING STRESS = _____ * = _____ ksi

CIRCUMFERENTIAL σ_θ

$\frac{PR_m}{T}$ * = _____ *

= _____ * = _____ ksi

= _____ * = _____ ksi

NOZZLE NO. _____

SHELL LOAD CASE _____

ANALYSIS POINT _____

COMPUTATION SHEET FOR LOCAL STRESSES IN CYLINDRICAL SHELLS

SEQUENCE _____

ITEM NO. _____

BY _____ DATE _____

CHK'D _____ DATE _____

Tables 2.10.1-16 to 21 summarize the resulting local membrane stresses and bending stresses for the various loading conditions. These local stresses are combined with the finite element results at the same locations from Section 2.10.1.3 above and compared with allowables in Section 2.6.

Tables 2.10.1-22 and 23 list the total stresses at all Figure 2.10.1-15 locations which includes the Section 2.10.1.2 finite element results and the local stresses at the trunnion locations from this section for the 3 g lifting and tie down load cases discussed in Section 2.5. Note that the stresses do not exceed the 30,000 psi yield strength of the 304 stainless steel at any location.

TABLE 2.10.1-16

LOCAL STRESSES AT TRUNNION/CASK BODY INTERFACE - CASK —

HORIZONTAL WITH 1 G VERTICAL LOADING

LOCATION		MEMBRANE STRESSES (PSI)		BENDING STRESSES (PSI)	
		MERIDIONAL SM	HOOP SH	MERIDIONAL SBM	HOOP SBH
CONTAINMENT	1				
	2				
	3				
	4				
	5				
	6				
	7				
	8				
	9				
	10				
	11				
	12				
NON-CONTAINMENT	13				
	14				
	15				
	16				
	17				
	18	98	57	440	810
	19				
	20				
	21				
	22	65	38	293	538
	23				
	24				
	25				

TABLE 2.10.1-17

LOCAL STRESSES AT TRUNNION/CASK BODY INTERFACE - WITH VIBRATION LOADING

LOCATION		MEMBRANE STRESSES (PSI)		BENDING STRESSES (PSI)	
		MERIDIONAL SM	HOOP SH	MERIDIONAL SBM	HOOP SBH
CONTAINMENT	1				
	2				
	3				
	4				
	5				
	6				
	7				
	8				
	9				
	10				
	11				
	12				
NON-CONTAINMENT	13				
	14				
	15				
	16				
	17				
	18	434	291	1089	1638
	19				
	20				
	21				
	22	415	326	1036	1475
	23				
	24				
	25				

TABLE 2.10.1-18

LOCAL STRESSES AT TRUNNION/CASK BODY INTERFACE - WITH SHOCK LOADING

LOCATION		MEMBRANE STRESSES (PSI)		BENDING STRESSES (PSI)	
		MERIDIONAL SM	HOOP SH	MERIDIONAL SBM	HOOP SBH
CONTAINMENT	1				
	2				
	3				
	4				
	5				
	6				
	7				
	8				
	9				
	10				
	11				
	12				
NON-CONTAINMENT	13				
	14				
	15				
	16				
	17				
	18	2345	1572	5943	8983
	19				
	20				
	21				
	22	2229	1899	6013	8027
	23				
	24				
	25				

TABLE 2.10.1-19

LOCAL STRESSES AT TRUNNION/CASK BODY INTERFACE - 3 G LIFTING LOAD (CASK VERTICAL)

	LOCATION	MEMBRANE STRESSES (PSI)		BENDING STRESSES (PSI)	
		MERIDIONAL SM	HOOP SH	MERIDIONAL SBM	HOOP SBH
CONTAINMENT	1				
	2				
	3				
	4				
	5				
	6				
	7				
	8				
	9				
	10				
	11				
	12				
NON-CONTAINMENT	13				
	14				
	15				
	16				
	17				
	18	1734	4860	13073	7848
	19				
	20				
	21				
	22	0	0	0	0
	23				
	24				
	25				

TABLE 2.10.1-20

LOCAL STRESSES AT TRUNNION/CASK BODY INTERFACE - 3 G LIFTING LOAD (CASK HORIZONTAL)

LOCATION		MEMBRANE STRESSES (PSI)		BENDING STRESSES (PSI)	
		MERIDIONAL SM	HOOP SH	MERIDIONAL SBM	HOOP SBH
CONTAINMENT	1				
	2				
	3				
	4				
	5				
	6				
	7				
	8				
	9				
	10				
	11				
	12				
NON-CONTAINMENT	13				
	14				
	15				
	16				
	17				
	18	1642	920	5752	10720
	19				
	20				
	21				
	22	1642	920	5752	10720
	23				
	24				
	25				

TABLE 2.10.1-21

LOCAL STRESSES AT TRUNNION/CASK BODY INTERFACE - WITH TIE DOWN LOADING

LOCATION		MEMBRANE STRESSES (PSI)		BENDING STRESSES (PSI)	
		MERIDIONAL SM	HOOP SH	MERIDIONAL SBM	HOOP SBH
CONTAINMENT	1				
	2				
	3				
	4				
	5				
	6				
	7				
	8				
	9				
	10				
	11				
	12				
NON-CONTAINMENT	13				
	14				
	15				
	16				
	17				
	18	6449	4402	14629	20820
	19				
	20				
	21				
	22	6958	6579	20763	23229
	23				
	24				
	25				

TABLE 2.10.1-22

STRESSES DUE TO TIE DOWN LOAD INCLUDING LOCAL STRESSES AT TRUNNION/CASK BODY INTERFACE

	LOCATION	MEMBRANE STRESSES (PSI)		BENDING STRESSES (PSI)	
		MERIDIONAL SM	HOOP SH	MERIDIONAL SBM	HOOP SBH
CONTAINMENT	1	811	918	-4627	-6551
	2	484	971	1106	-577
	3	-639	-1123	-6421	-1688
	4	-1055	-1397	5746	1718
	5	-2081	-1865	5	-16
	6	-1881	-1164	52	-14
	7	-1498	-909	-23	-50
	8	-1566	-1150	-64	-53
	9	-1603	-1061	316	76
	10	-1192	91	-1100	-327
	11	366	561	-939	-250
	12	303	222	116	141
NON-CONTAINMENT	13	-1358	-1346	709	-444
	14	-1275	-1072	607	40
	15	-587	-865	787	237
	16	-597	646	-3122	-937
	17	2788	315	2638	782
	18	8977	6132	14554	20757
	19	2960	1558	-85	-90
	20	3401	1240	-83	-116
	21	3204	1183	-54	-89
	22	6363	7471	20752	23183
	23	-240	104	-3051	-914
	24	-58	161	-1122	55
	25	-212	-64	1673	1655

TABLE 2.10.1-23

STRESSES DUE TO 3 G LIFTING LOAD INCLUDING LOCAL STRESSES AT TRUNNION/CASK BODY INTERFACE

LOCATION		MEMBRANE STRESSES (PSI)		BENDING STRESSES (PSI)	
		MERIDIONAL SM	HOOP SH	MERIDIONAL SBM	HOOP SBH
CONTAINMENT	1	-48	11	11	-6
	2	-35	99	-82	-36
	3	-35	15	-240	-60
	4	-39	-11	250	71
	5	-44	-127	13	-6
	6	47	-16	25	-9
	7	216	136	-14	-28
	8	133	2	-36	-30
	9	84	-175	80	13
	10	79	132	-112	-35
	11	57	127	-40	-19
	12	23	-22	-2	-3
NON-CONTAINMENT	13	14	20	2	-1
	14	60	165	-76	-20
	15	52	164	-169	-50
	16	25	117	-245	-73
	17	46	120	118	30
	18	1513	1468	5809	10715
	19	76	321	-26	-43
	20	270	252	-45	-64
	21	109	324	-33	-50
	22	1461	1537	5828	10720
	23	2	133	147	45
	24	15	137	41	12
	25	-71	12	4	-15

2.10.1.3 LID BOLT ANALYSIS

The TN-RAM lid closure arrangement is shown in Figure 2.10.1-16. The 2.5 inch thick lid is bolted directly to the end of the containment vessel body by 16 high strength 1 1/2 inch diameter bolts. The center of the lid is recessed into the vessel flange with adequate clearance for ease of insertion and removal. Close fitting alignment pins ensure that the lid is centered in the vessel.

The lid bolt is shown in Figure 2.10.1-17. Note that the material is ASME SA-564, Type 630 Condition H1100 which has a minimum yield strength of 115,000 psi at room temperature. The bolt has a 4.88 inch long undercut shank 1.32 inches in diameter. The lid closure flange and bolt arrangement is shown in Figure 2.10.1-18. The bolts are designed to be preloaded at assembly to seat the seals against the 30 psi maximum normal operating pressure and to withstand all normal and accident loadings without yielding. 2

Applied Loading

The most severe inertial loadings on the containment vessel occur during the 30 foot drop accident. The corner drop orientation with the lid end impacting produce tensile loading of the bolts due to inertial loads of the lid and payload. The overall system free body diagram of the entire packaging during a corner drop on the lid end is shown in Figure 2.10.1-19. The case shown is the most severe corner impact case from Appendix 2.10.2 with the containment vessel approaching an upright orientation (axis at 85°). The axial deceleration value is 81 g.

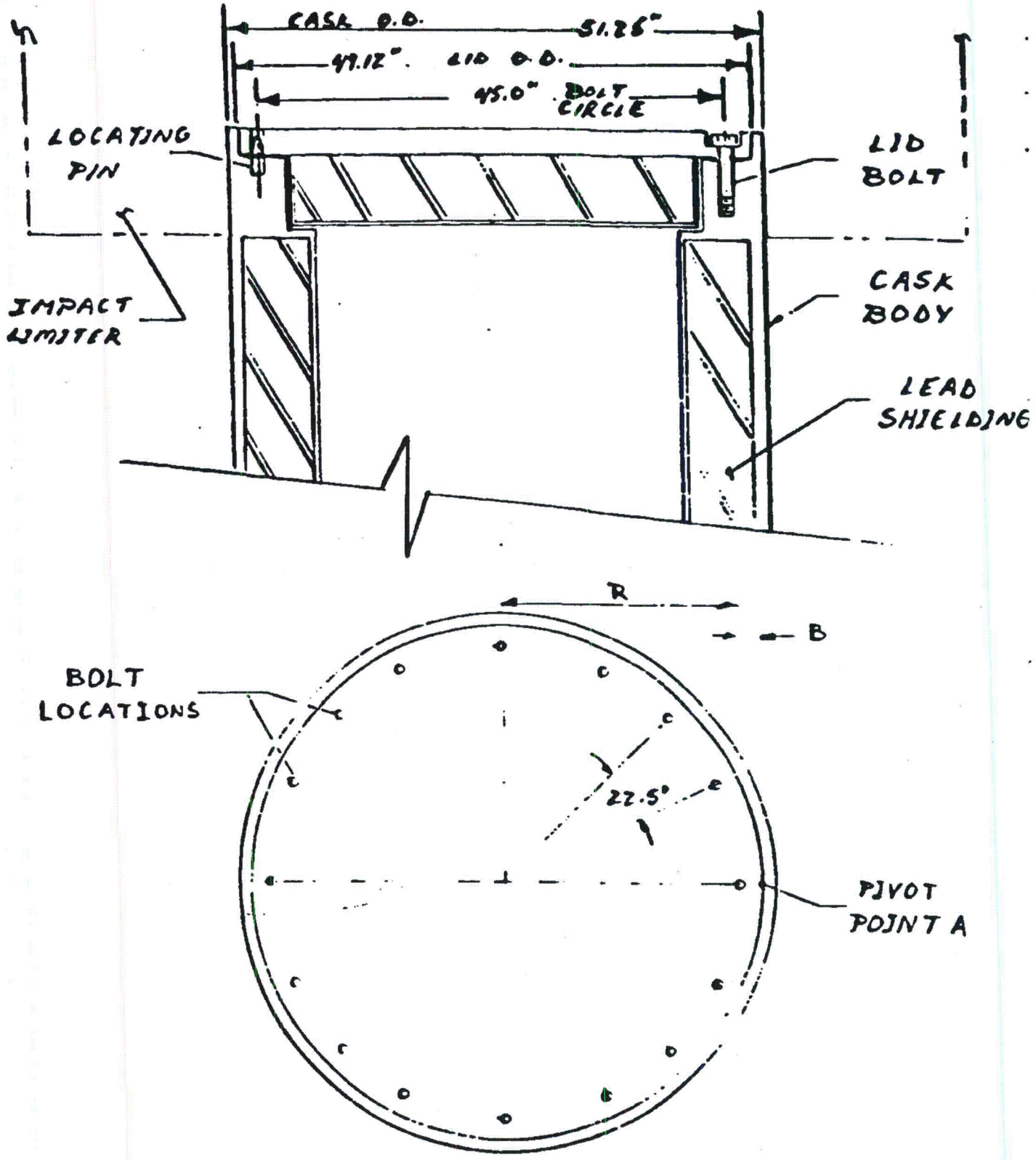

FIGURE 2.10.1-16

TN-RAM LID CLOSURE

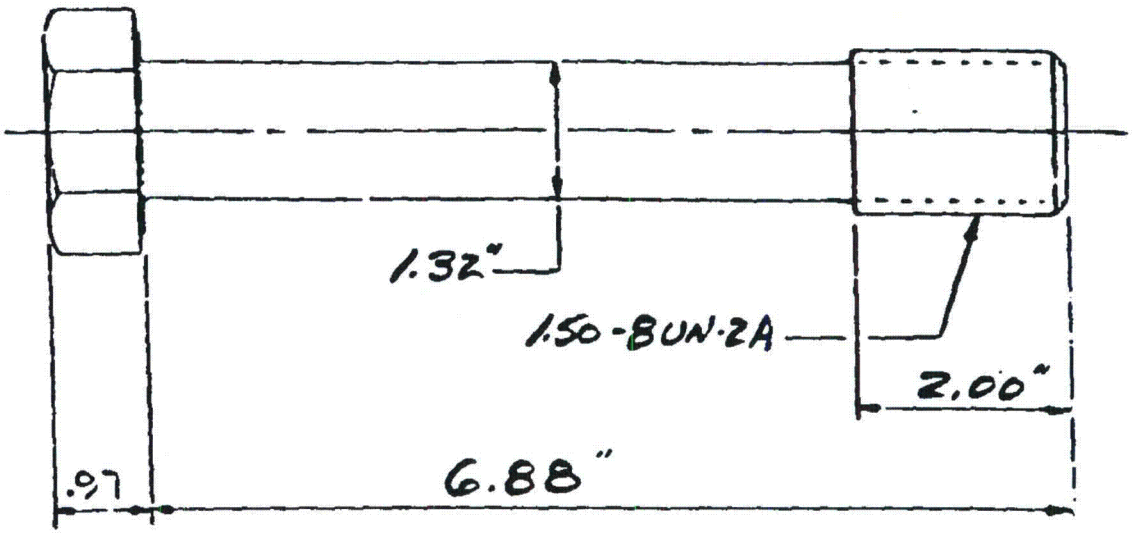

FIGURE 2.10.1-17

TN-RAM LID BOLT

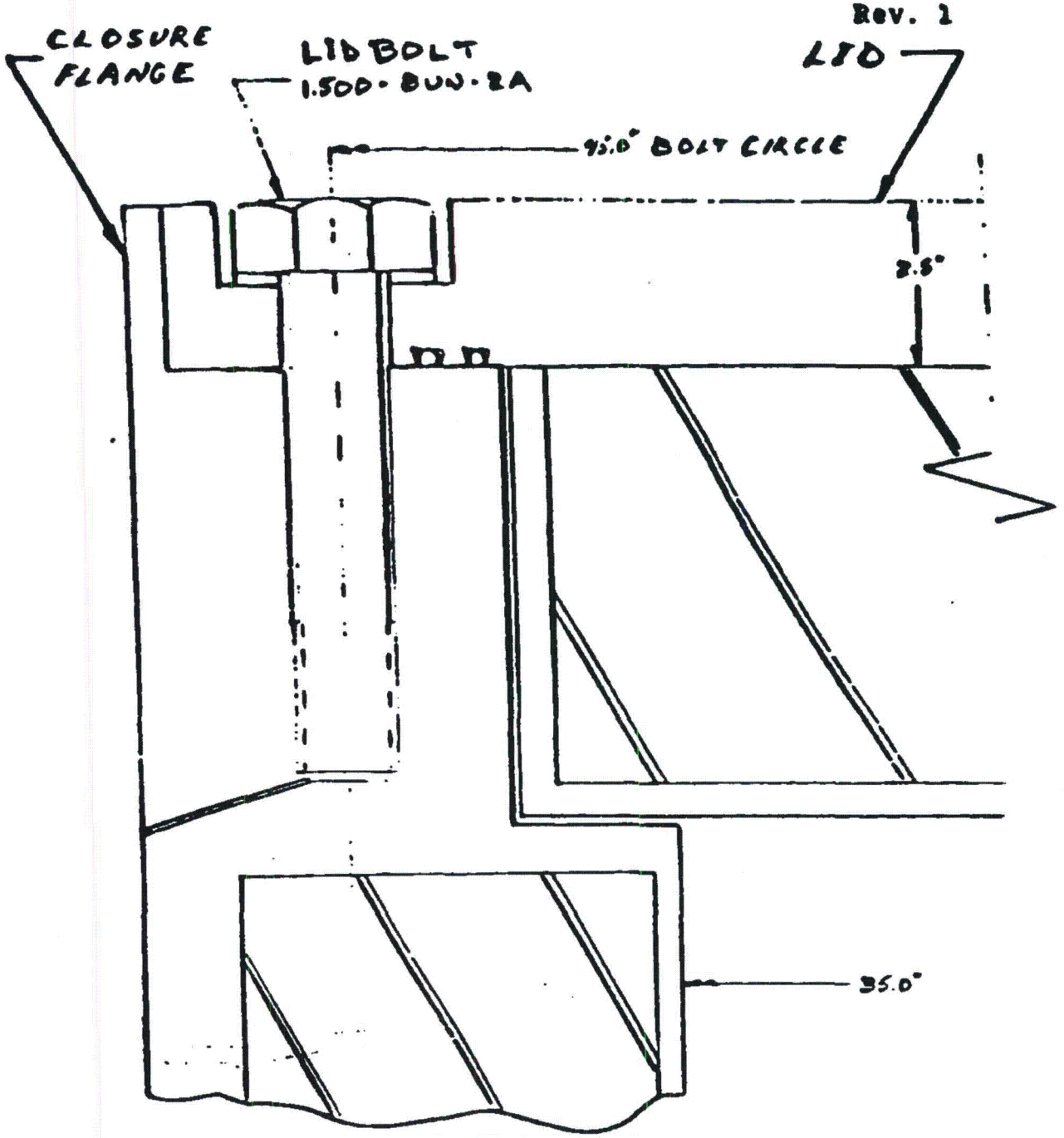

FIGURE 2.10.1-18

TN-RAM LID BOLT ARRANGEMENT

W_I : WEIGHT OF INTERNALS
W_L : WEIGHT OF LID
G : DECELERATION ⊥ TO IMPACT SURFACE
G_A : AXIAL COMPONENT OF G
G_L : LATERAL COMPONENT OF G
R_I : IMPACT FORCE

W_I = 9,500 lb.
W_L = 4,700 lb.

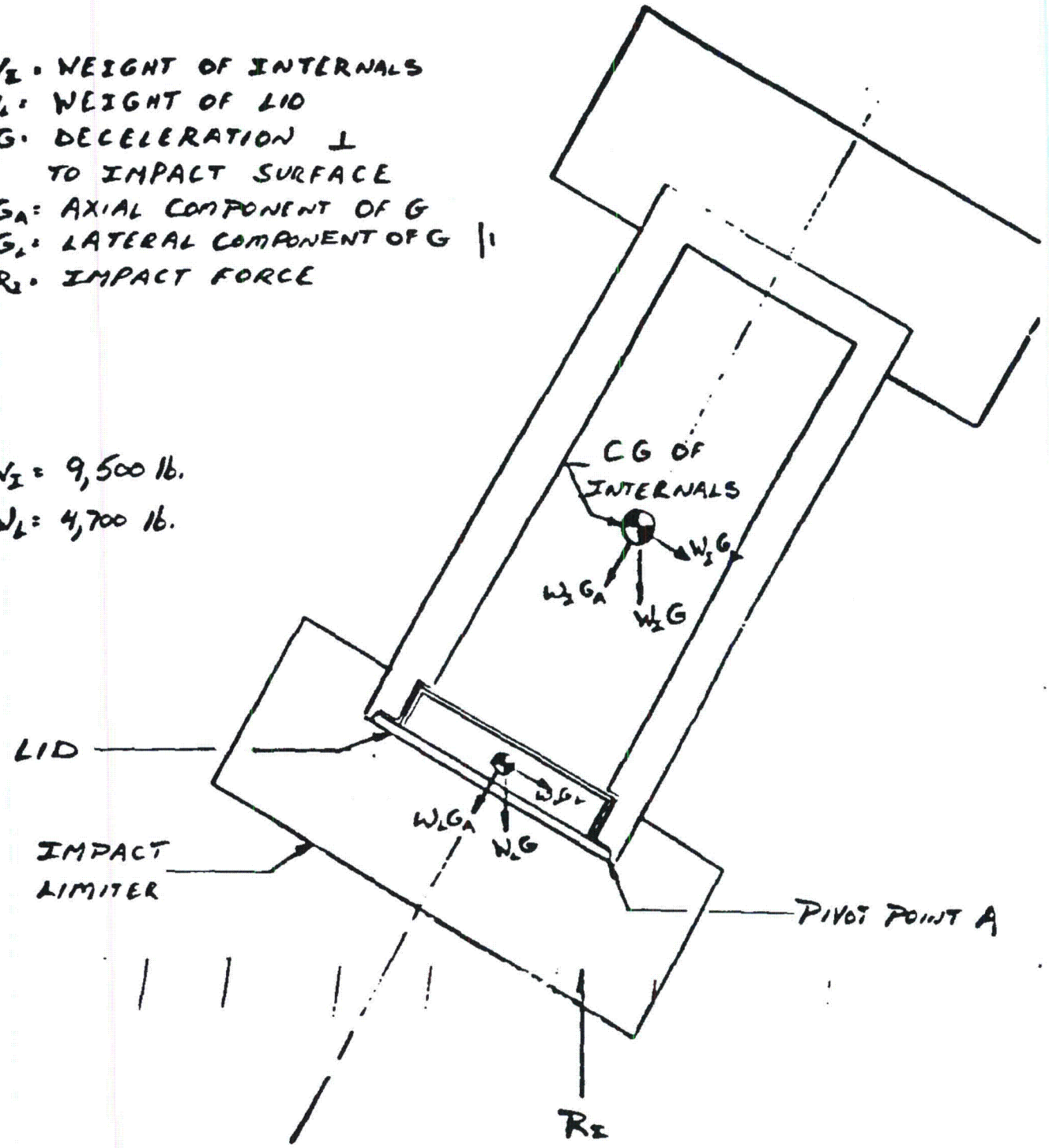

FIGURE 2.10.1-19

IMPACT FORCE AND INERTIA LOADS ACTING ON TN-RAM LID
FREE BODY DIAGRAM

As can be seen in Figure 2.10.1-19, the impact force is directed upward from the "footprint" on the impact limiter through the edge of the lid toward the center of gravity. It is conservatively assumed that the impact force passes through the pivot point shown between the lid and vessel, holding the lid against the vessel at this one point. The force is actually acting toward the center of the lid from the pivot point tending to seat the lid against the vessel, but this seating effect is conservatively neglected.

The various inertial forces are also shown in Figure 2.10.1-19. The external impact force is assumed to be perpendicular to the target and therefore at a 5° angle from the containment vessel axis. Therefore the resultant inertial loads on each component are oriented at a 5° angle from the containment vessel axis. The axial load of the internals and the lid are resisted by the lid bolts. The lateral inertial load of the lid is resisted by the shoulder of the closure flange.

The axial forces applied to the lid are calculated below. The reaction force is assumed to hold the lid against the flange at point A producing rigid body rotation of the lid about point A. This rigid body rotation is resisted by the lid bolts and produces stress distribution dependent on the lid bolting pattern taken abou point A.

The axial loads on the lid are:

<u>Inertial Loads, lbs.</u>

$W_I \times G_A$ = 9,500 x 81.0 = 769,500 lbs.

$W_L \times G_A$ = 4,700 x 81.0 = 380,700 lbs.

Axial Pressure Load, lbs.

$P_A = A \times 30 = 165,000$

The moments on the lid about point A due to the above loadings are:

Due to Axial Loads

$W_I G_A (R + B) = 18.9 \times 10^6$

$W_L G_A (R + B) = 9.3 \times 10^6$

28.2×10^6 in-lbs

where R is the bolt circle radius and B is the distance from the bolt circle to pivot point A as shown in Figure 2.10.1-16.

Due to Internal Pressure

$39,400 (R + B) = .970 \times 10^6$ in-lbs

The total unseating moment (counter-clockwise) on the lid about point A due to all of these forces is then 29.2×10^6 in-lbs.

Bolt Analysis

The lid bolts must hold the lid onto the containment vessel and resist the above unseating moment. The lid bolts are analyzed for two cases: one case considers preload and the other case ignores preload effects to show that the actual level of preload is not

critical. Figure 2.10.1-20 shows the lid bolt reaction forces on the lid as it separates slightly from the containment vessel body (except at point A) and rotates counter-clockwise about A. The separation distance is assumed to be zero at point A and maximum on the extreme opposite edge of the lid.

Case (a) on Figure 2.10.1-20a ignores the effects of preload. Bolt elongation occurs as a result of this slight lid separation and the elongation is therefore proportional to the distance from point A. The bolt load then is also proportional to the distance from A with the maximum load, F_B, on the bolt located farthest from point A. Case (b) shows the effect of preload. Each bolt load is equal to the preload, F_p, before separation. After separation every bolt is stretched as a result of this separation. The increase in bolt load above the preload value is then proportional to the distance from A. The total bolt load is then F_p plus the increase in bolt load. The highest loaded bolt is loaded to F_p plus ΔF_B and is the bolt farthest from point A.

Bolt Stresses - Neglecting Preload

Inertial Load Stresses

2

The lid bolt stress distribution resulting from the inertial loads about point A can be described with the equation (See Figure 2.10.1-21):

$$\sigma_i = \frac{M \times C_i}{I_{aa}}$$

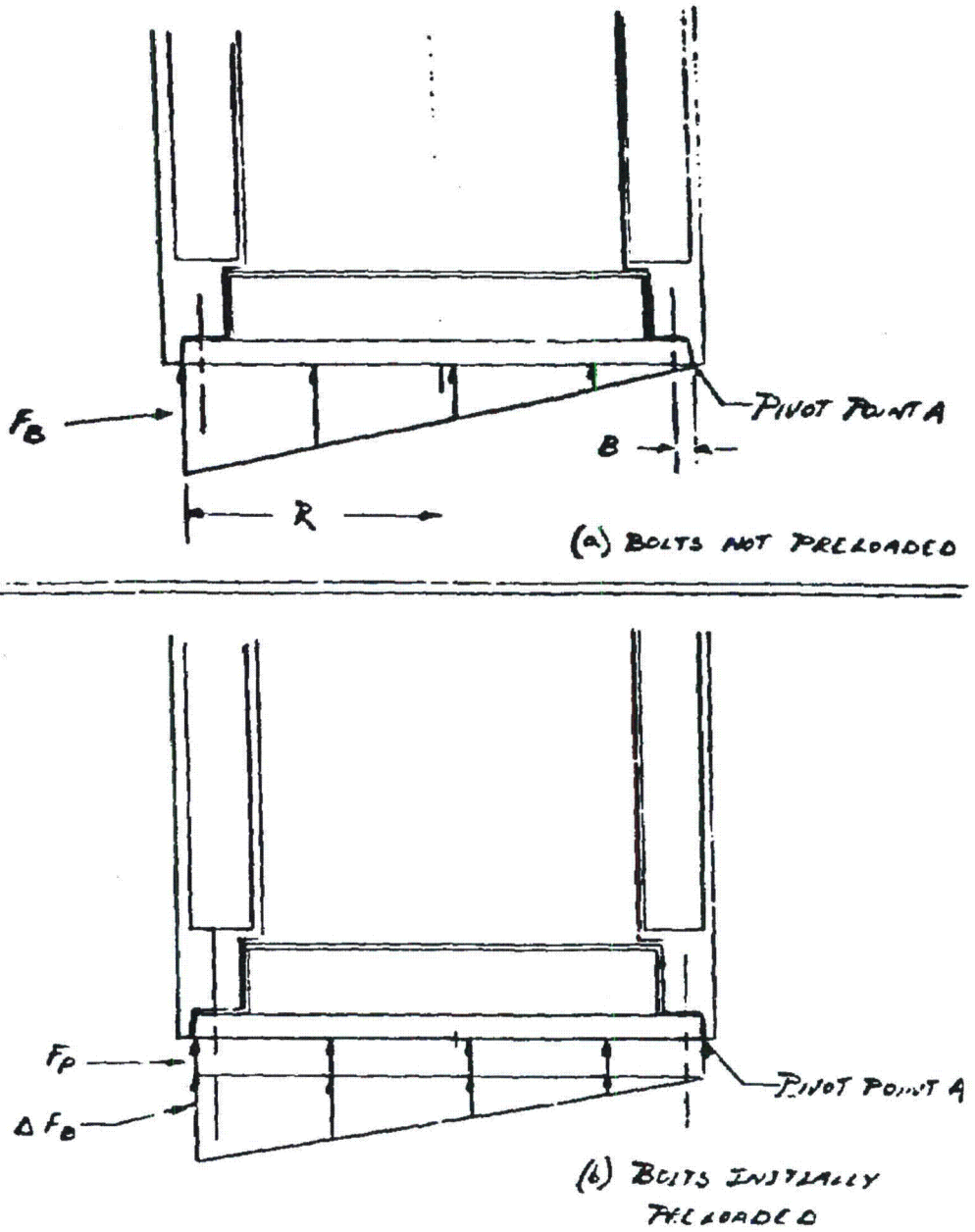

FIGURE 2.10.1-20

LID BOLTS REACTING AXIAL INERTIA LOADS

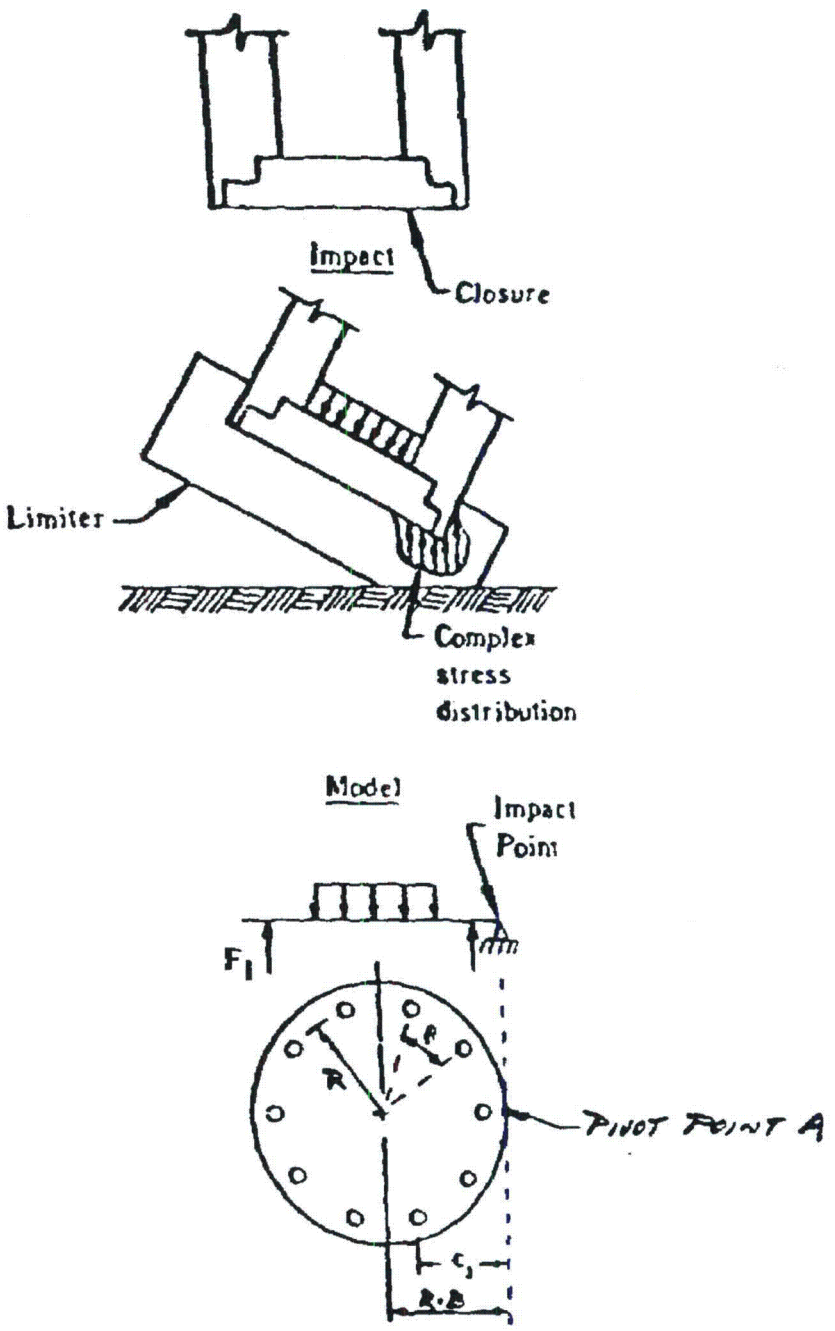

FIGURE 2.10.1-21

LID BOLT ANALYSIS MODEL

where

M = moment due to inertial loads about point A (in-lb)

C_i = moment arm of bolt i about point A (in)

I_{aa} = moment of inertia of bolt group about point A (in^4)

Moment of inertia of bolt group about point A is calculated as follows: (NUREG/CR-3966 "Methods for Impact Analysis of Shipping Containers".)

$$I_{aa} = \frac{N(R)^2 A_b}{2} + N A_b (R + B)^2 = 18,771 \text{ in}^4$$

where

N = number of bolts = 16

R = bolt circle radius = 22.5 in.

A_b = bolt tension area = 1.37 $in.^2$

B = distance from closest bolt to Pivot Point A, 2.06 in.

$R + B$ = lid outside radius = 24.56 in.

Maximum bolt stress occurs when

$$C_i = 2R + B = 47.06 \text{ in.}$$

Therefore

$$\sigma_{i(max)} = \frac{29.2 \times 10^6 \times 47.06}{18,771}$$

$$\sigma_{i(max)} = 73.2 \text{ ksi}$$

2

Bolt Stresses - Including Preload Effects

The bolts will be preloaded to a stress value of 28,000 psi. The preload in each bolt, F_p, is 28,000 x A_B or 28,000 x 1.37 = 38,360 lb. The resultant total load in all 16 bolts is F_p x 16 = 38,360 x 16 = .610 x 10^6 lbs. The resultant load vector (of the total bolt preload force) is located normal to the center of the lid. The clockwise seating moment of this force about point A is M_{pr} = 16 F_p (R + B) = 15.0 x 10^6 in lb.

The applied moment about point A of 29.2 x 10^6 in lb exceeds the preload seating moment so the lid bolts will be stretched beyond the preload strain. The applied moment exceeds the preload seating moment by 29.2 x 10^6 - 15.0 x 10^6 = 14.2 x 10^6 in lb.

The increased tensile stress above preload in the highest loaded bolt is then:

$$\sigma_i = \frac{(\text{Applied moment} - \text{Preload moment})(47.06)}{I_{aa}}$$

$$= \frac{14.2 \times 10^6 \times 47.06}{18,771}$$

$$= 35.6 \text{ ksi}$$

3

The total bolt stress with preload then is:

$$\sigma_T = 28.0 + 35.6$$

$$= 63.6 \text{ ksi}$$

3

This is slightly less than the 73.2 ksi stress obtained when preload is neglected. 3

Differential Thermal Expansion Stresses

The thermal coefficient of expansion of the bolt material is less than the lid material thermal coefficient of expansion. This introduces some tensile stresses in the lid bolts. However, the lid bolts and lid in the area of the bolts are basically at the same temperature during normal and thermal accident conditions because of the insulation provided by the impact limiter. Therefore there are no additional bolt stresses due to temperature differences between the lid and lid bolts.

The bolt stress due to a difference in thermal coefficients of expansion for the normal condition of transport are calculated as follows:

$$\sigma_e = E_b \times \Delta\alpha \times \Delta T$$

where

σ_e = tensile bolt stress due to differential thermal expansion

E_b = Young's Modulus for bolt at 164°F
$= 27.8 \times 10^6$ psi

$\Delta\alpha = \alpha_{lid} - \alpha_{bolt}$

and $\alpha_{lid} = 8.7 \times 10^{-6}$ in/in/°F @ 164°F

$\alpha_{Bolt} = 5.89 \times 10^{-6}$ in/in/°F @ 164°F

Note: The values used for E and α are interpolated based on Table 2.3-2 of Chapter 2.0. The temperature of the lid and bolts of 164°F is obtained from Table 3-1 of Chapter 3.0.

$\Delta T = T_{NC} - Tamb$

and T_{NC} = normal condition temperature of 164°F

Tamb = ambient temperature, 65°F

Therefore

$$\sigma_e = (27.8 \times 10^6)\ (8.7 - 5.89) \times 10^{-6}\ (164-65)$$

$$= 27.8 \times 2.81 \times 99$$

$$= 7,734 \text{ psi}$$

The bolt stresses for the thermal accident conditions are calculated in a similar manner. The maximum temperature in the lid during the thermal accident is 221°F as given in Table 3.7 of Chapter 3.0. Interpolating the values in Table 2.3-2, the material properties values at 221°F are

$E_b = 27.48 \times 10^6$ psi
$\alpha_{lid} = 8.83 \times 10^{-6}$ in/in/°F
$\alpha_{bolt} = 5.90 \times 10^{-6}$ in/in°F

Therefore

$$\sigma_e = (27.48 \times 10^6)(8.83 - 5.90) \times 10^{-6}(221-65)$$
$$= 27.48 \times 2.93 \times 156$$
$$= 12,560 \text{ psi}$$

Total Bolt Stress

The stress due to the thermal accident of 12.56 ksi is less than the inertial load stress of 73.2 ksi for the corner drop and is therefore not critical.

The bolt stress due to differential thermal expansion for the normal condition of transport can be conservatively added to the inertial load stresses for the corner drop to obtain the maximum total bolt stress.

Therefore the maximum total bolt stress, σ_T, is

$$\sigma_T = \sigma_i + \sigma_e$$
$$= 73.2 + 7.7$$
$$= 80.9 \text{ ksi}$$

The factor of safety against yielding is:

$$F.S._{yield} = \frac{115}{80.9} = 1.42$$

The factor of safety over ultimate stress is:

$$F.S._{ultimate} = \frac{140}{80.9} = 1.73$$

Closure Flange Shoulder Analysis

Transverse lid deceleration loads are resisted by the closure flange shoulder during all normal and accident conditions. The shoulder thickness at the base has a shear area equal to

$$\text{Shear Area} = \frac{(51.25)^2-(49.25)^2}{4}\pi = 158 \text{ in}^2$$

For conservatism, it is assumed only 120° arc of the shoulder is effective. Effective shear is:

$$\text{Effective Shear} = \frac{120}{360}(158) = 53 \text{ in}^2$$

Normal Conditions of Transport

Maximum transverse deceleration loads during normal conditions occurs during hypothetical one foot horizontal drop. The maximum deceleration is 36.3 g's. (Table 2.10.2-5 of Appendix 2.10.2)

Total Force = 36.3 x wt of lid = 36.3 (4700) = 170,600 lbs.

$$\text{Average Shear Stress} = \frac{170,600}{53} = 3,240 \text{ psi}$$

$$\text{Allowable Average Shear} = S_y/2 = 30,000/2 = 15,000 \text{ psi}$$

$$\text{Factor of Safety} = \frac{15,000}{3,240} = 4.6$$

Hypothetical Accident Conditions

Maximum transverse deceleration load during accident conditions of 140 g's occurs for the near horizontal 30 foot drop (i.e. 10°). The total force on the shoulder equals

Shear force = 140 x wt. of lid
= 140 (4,700) = 658,000 lbs.

Average shear stress across shoulder = $\frac{658,000}{53}$ = 12,415 psi

Allowable average shear = Ultimate stress of closure flange material/2

= $\frac{75,000}{2}$ = 37,500

Factor of Safety = $\frac{37,500}{12,415}$ = 3.0

Conclusions

The maximum stress in the lid bolts during the 30 foot drop is shown to be 73.2 ksi ignoring preload in the analysis and 63.6 ksi considering the preload. Therefore preload is not critical in the evaluation. This is an acceptable stress level (below yield) in these bolts (A-564, Type 630, Condition H1100) which have a minimum yield strength of 115,000 psi. Furthermore, this is the stress level at two points in the single highest loaded bolt using a very conservative approach to the development of the free body diagram. Lid shoulder stresses during both normal and accident conditions provide large margins of safety of resisting transverse lid deceleration loads.

APPENDIX 2.10.2
STRUCTURAL ANALYSIS OF IMPACT LIMITERS

2.10.2.1 INTRODUCTION

This appendix presents the details of the structural analysis of the TN-RAM impact limiters. The impact limiters are designed to absorb the kinetic energy resulting from the one (1) foot and thirty (30) foot normal and hypothetical accident free drop events specified by 10 CFR 71. Redwood and balsa wood are used as the primary energy absorption material(s) in the impact limiters. A sketch of the impact limiter is shown in Figure 2.10.2-1. A functional description of the impact limiters is given in Section 2.10.2.2. The impact limiter design criteria are described in Section 2.10.2.3.

A computer model of the TN-RAM Packaging was developed to perform a system dynamic analysis during the impact after the 30 foot drop accident. The model was developed for use with the ADOC (Acceleration Due To Drop On Covers) computer code described in detail in Section 2.10.2.5 which determines the deformation of the impact limiters, the forces on the containment and the packaging deceleration due to impact on an unyielding surface. Numerous cases were run to determine the effects of the wood properties and initial drop angle. A description of the computer model, input data, the ADOC computer code, analysis results and conclusions are given in Sections 2.10.2.4 through 2.10.2.5. The forces and decelerations calculated by ADOC have been used in the cask body structural analysis which is presented in detail in Appendix 2.10.1. Test

Security-Related Information
Figure Withheld Under 10 CFR 2.390

IMPACT LIMITER

FIGURE 2.10.2-1

programs on wood filled limiters of similar designs have been completed and are discussed in Appendix 2.10.3. Test results indicate that ADOC predicts conservatively high deceleration values and crush forces.

The dynamic analysis of the TN-RAM for the one foot normal condition free drop is presented in Section 2.10.2.6. The analysis of the impact limiter attachments and the analysis of the impact limiter under normal pressure fluctuations are described in Sections 2.10.2.7 and 2.10.2.8, respectively.

2.10.2.2. DESIGN DESCRIPTION

The impact limiters absorb energy during impact events by crushing of balsa and redwood. The size, location and orientation of each wood block is selected to provide protection for the cask during all normal conditions of transport and hypothetical accident conditions.

The top and bottom impact limiters are identical and interchangeable. Each has a diameter of 91.75 inches and a height of 34.62 inches. The inner and outer shells are Type 304 stainless steel joined by radial gussets of the same material. The gussets limit the stresses in the 0.125 in. thick steel outer cylinder and end plates due to pressure differentials caused by elevation and temperature changes during normal transport and provide wood confinement during impact. The metal structure positions, supports, confines and protects the wood energy absorption material. The metal structure does contribute to the energy absorbing capability of the impact limiter. However, the contribution for a side drop or oblique angles is negligible because contact starts at a single point with the unyielding surface (target) and initiates buckling of a single gusset. After the drop event is complete, relatively few gussets are buckled. Each limiter has 13 wood compartments: a central circular region 24 inch diameter surrounded by 12 radial pie shaped compartments.

The region of the impact limiter which is backed-up by the cask body is filled with balsa wood orientated with the grain direction perpendicular to the end of the cylindrical cask (See Figure 2.10.2-1). The material and grain orientation are selected to provide acceptably low deceleration to prevent lead slump during impact after

the thirty foot end drop. A 2.0 inch layer of balsa wood with the grain parallel to the end of the cylindrical cask is provided on the outer face of the impact limiter to minimize decelerations under the one foot end drop.

A 10.12 inch wide ring of redwood (consisting of 12 segments or blocks of wood) is located in the sides of the pie shaped compartments which surround the end of the cylindrical surface of the cask with the grain direction oriented radially. This ring of redwood absorbs most of the kinetic energy during a side drop. Redwood was selected for this portion of the impact limiter because of its high crush strength and hence the ability of a small amount of wood to absorb a large amount of energy in a relatively short crush distance.

The corners of the pie shaped compartments are filled with redwood and balsa blocks. A 14.75 inch section of redwood is located next to the side redwood and a 9.75 inch block of balsa wood is located in the outer corner. The grain orientation in the redwood block is parallel to the side of the cask body and that in the balsa block is parallel to the end (radial). The primary function of the redwoood block is energy absorption during corner drops while the balsa wood limits the decelerations to acceptable levels during the one foot normal condition end drop.

All wood blocks used in the impact limiters are composed of individual boards glued together with a Phenol Resorcinol Adhesive. This adhesive was selected for its superior strength and moisture resistance. The glue is waterproof up to a temperature of 200°F. The adhesive used conforms to the requirements of Federal

Specification MMM-A-188b. The wood blocks are assembled and glued together in accordance with an approved QA procedure. Minimum properties of the adhesive are listed in Table 2.10.2-1. Ranges of shear and tensile strengths of each type of wood are also listed. The adhesive is significantly stronger than any of the wood used in the limiter in terms of shear and tension strength. Therefore the boards or blocks of wood will not fail along the glue joints.

The other mechanical properties of the wood used in the analysis of the impact limiters are shown in Table 2.10.2-2. The crush stress properties used cover the range of expected values for the density and moisture content specified in the procurement specification. These ranges also cover the expected variation in wood properties over the operating temperature range of interest; i.e., -20°F to 165°F.* During procurement, wood samples are tested for moisture content and crush stress in accordance with an approved sampling plan.

If the density and moisture content are not within the specified range, the wood blocks from which samples are taken will be rejected.

* Von Riessman, W. A. and Guiss, T. R. The Effects of Temperature on the Energy-Absorbing Characteristics of Redwood, Sandia Laboratories SAND-77-1509, Aug. 1978

Knoell, A. C., Environmental and Physical Effects in the Response Balsa Wood in an Energy Dissipation, Jet Propulsion Laboratory, Technical Report No. 32-944, June 15, 1966

TABLE 2.10.2-1

MECHANICAL PROPERTIES OF WOOD AND WOOD ADHESIVE

Minimum Properties of Phenol Resorcinol Adhesive

Shear Strength by Compression Loading	2,800 lbs/in^2 (1)
Shear Strength by Tension Loading	340 lbs/in^2 (1)

Properties of Heavy Balsa (10-12 lb/ft^3)

Shear Strength Parallel to Grain	315-385 psi max. (2)
Tensile Strength Perpendicular to Grain	140-160 psi (2)

Properties of Redwood

Shear Strength Parallel to Grain	940 psi (3)
Tensile Strength Perpendicular to Grain	240 psi (3)

(1) Federal Specification MMM-A-188b

(2) Dreisback, J.F., Balsa Wood and Its Properties, Columbia Graphs, Columbia, CT 1952

(3) Marks Standard Handbook for Mechanical Engineers, Eighth Edition, pg. 6-124

For the end drop, all of the wood in the central part of the impact limiter that is directly "backed-up" by the cask body will crush. The wood in the corner and side of the limiter will tend to slide around the side of the cask since it is not supported or backed-up by the body and it will not crush or absorb energy as effectively as the wood that is backed-up. During the side or oblique drop the wood backed up by the cask will crush, while the wood beyond the end of the cask body will have a tendency to slide around the end of the cask. The analyses assume that the effectiveness of the portion of the wood that is not backed-up may be as small as 20% or as large as 80%. Effectiveness is defined as the actual crush force developed at the target by this material divided by the theoretical force required to deflect the material. The analysis also assumes a range of wood crush strengths. When determining maximum deceleration, the maximum crush strengths are used and the non backed-up material is assumed to be 80% effective. When determining crush depth, the minimum wood crush strengths are used and the non backed-up wood is considered to be only 20% effective.

Each impact limiter is attached to eight local lugs welded to the side of the cask using high strength bolts. The attachments have been sized to withstand the loads transmitted during a side drop. This analysis is described in Section 2.10.2.7 of this Appendix.

2.10.2.3 DESIGN CRITERIA

The outside dimensions of the impact limiter are sized to be well within federal and state highway height and width restrictions. The balsa and redwood distribution and densities have been selected to limit the maximum cask body inertia loads due to the one foot normal condition drop and the thirty foot hypothetical accident drop so that the design criteria specified for the containment boundary, the non containment structure and shielding (See Section 2.1) are met.

The welded stainless steel structure of the impact limiter is designed so that the wood is maintained in position and is confined during crushing of the impact limiters. The outer shell and gussets are designed to buckle and crush during impact. Local failure of the shell is allowed during impact limiter crushing. The welded stainless steel shell and its internal gussets are designed to withstand pressure differences and normal handling and transport loads with stresses limited to the material yield strength.

The impact limiters are designed to remain attached to the cask body during all normal and hypothetical accident conditions.

2.10.2.4 ANALYSIS FOR 30 FT FREE DROP ACCIDENT CONDITIONS

2.10.2.4.1 Approach

The kinetic energy due to the hypothetical 30 ft drop accident is absorbed by crushing of the impact limiters on the ends of the packaging. The limiters contain materials, i.e. balsa and redwood, which provide controlled deceleration of the packaging by crushing between the target surface and the cask body.

The applicable regulation, 10CFR71.73, requires that the packaging be oriented for the drop so that it strikes the target in a position for which maximum damage is expected. Dynamic impact analyses were performed for different packaging orientations using the ADOC computer code described in Section 2.10.2.5. This computer code has been validated by comparing its dynamic results with those from hand calculations for relatively simple problems, comparing its calculated force-deflection curves with those obtained from static crush tests, and by correlating dynamic results with actual measured cask behavior on other programs (see Appendix 2.10.3).

2.10.2.4.2 Assumptions and Boundary Conditions

The assumptions and boundary conditions are as follows:

1. The cask body is assumed to be rigid and absorbs no energy. This assumption is realistic since the design criteria of Section 2.1.2 limit metal deformations to small values. All of the impact energy is therefore assumed to be absorbed by the impact limiters.

2. The crushable material is one or several anisotropic materials. The different wood regions are modeled individually.

3. The crush strengths of the wood sections are obtained from the properties parallel to and perpendicular to the grain based on the orientation of the cask at impact.

4. Each wood region is modeled as a one dimensional elastic, perfectly plastic material up to a specific locking strain. After reaching the locking strain, the stress increases linearly with additional strain. The wood properties (modulus of elasticity, average crush strength, locking modulus, and locking strain) are taken from force-deflection curves of sample blocks of wood. Typical force-deflection curves for redwood and balsa are shown in Figures 2.10.2-1A and 2.10.2-1B. Since the locking strain varies from sample to sample, conservatively low locking strains of 80% for balsa and 60% for redwood are used.

5. The crush properties of the wood are varied with the initial angle of impact and do not change during the drop event being evaluated.

6. The cask and impact limiters are axisymmetric bodies.

7. The crushing resistances of the impact limiter shell and gussets have a negligible effect on the crush strength of the limiter and, therefore, a negligible effect on the impact forces and inertia loads.

---

*

FIGURE 2.10.2-1A

SAMPLE FORCE-DEFLECTION CURVE FOR BALSA

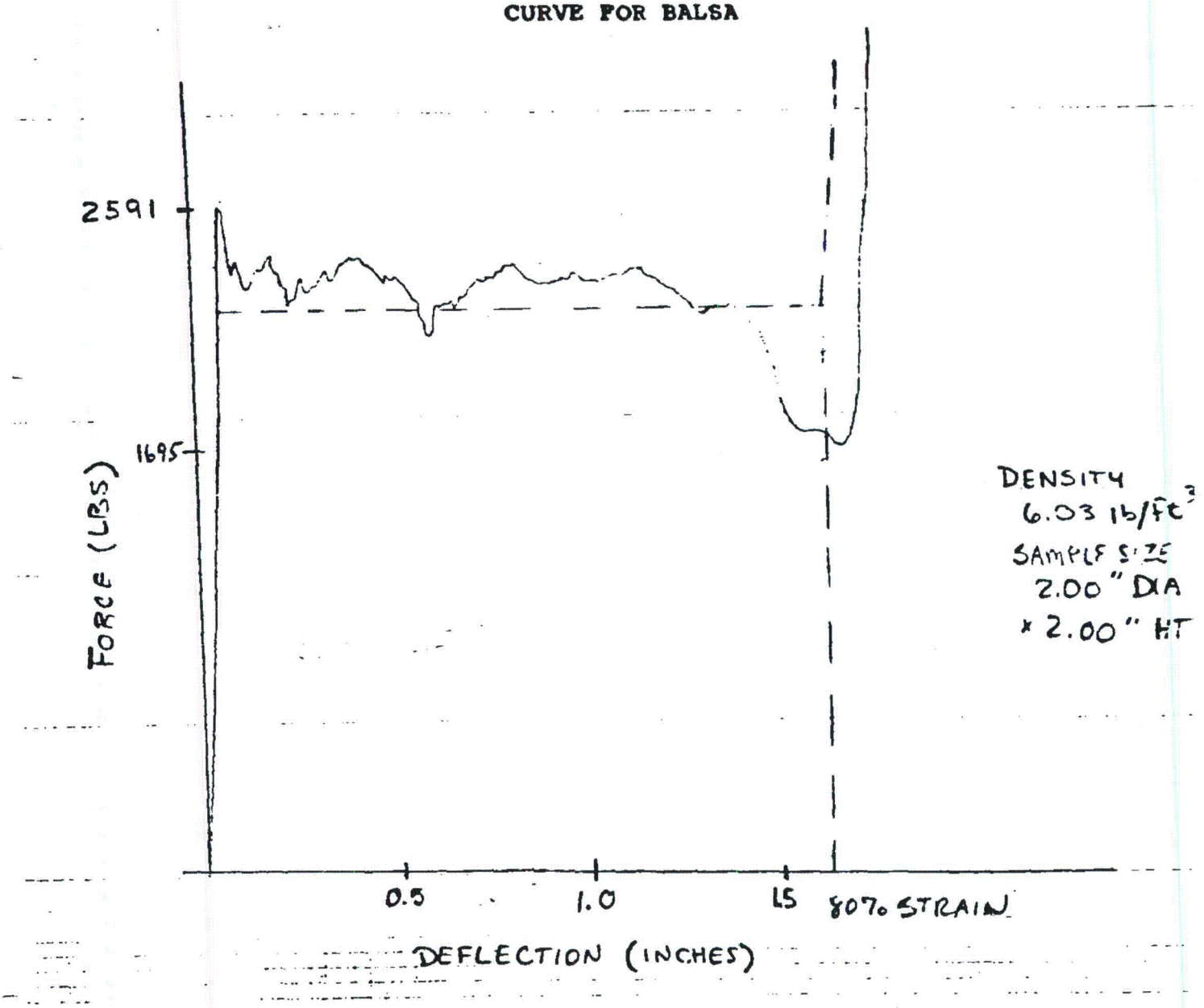

FIGURE 2.10.2-1B

SAMPLE FORCE-DEFLECTION CURVE FOR REDWOOD

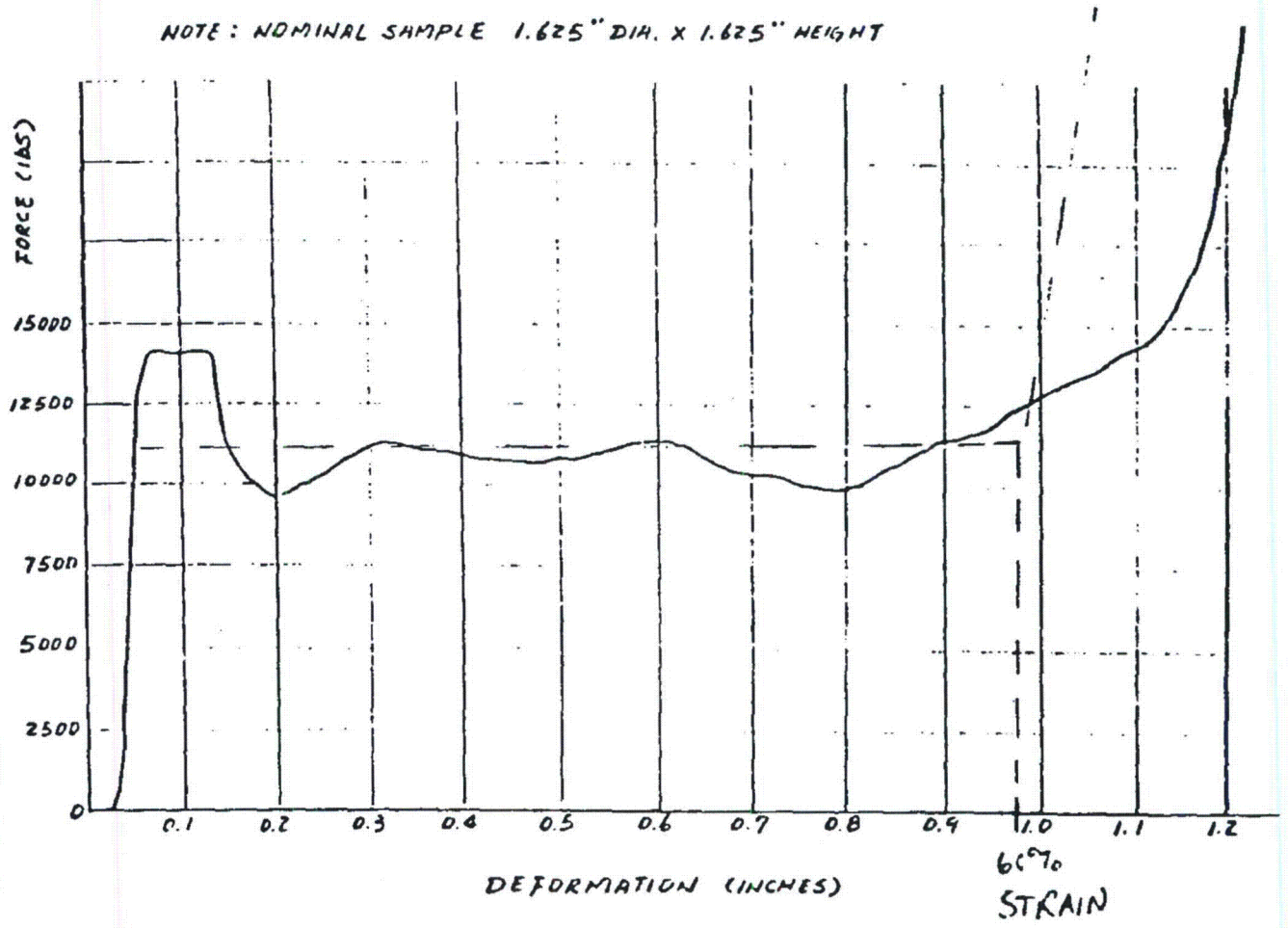

2.10.2.4.3 Packaging Dynamic Computer Model

Figure 2.10.2-2A illustrates the computer model used for all packaging orientations. Regions I, II, and III in the model are used to delineate regions where different impact limiter materials are used. It should be noted that the properties of the three regions have been designed by choosing wood types and orientations to accommodate the crush requirements of the three significant drop orientations. The crushable materials of Regions I, II, and III are selected to control the decelerations resulting from vertical, corner, and side drop orientations, respectively. Table 2.10.2-2 tabulates the wood properties that were used to describe the wood stress-strain behavior in the analysis.

A portion of the impact limiter crushable material is backed up by the cask body as it crushes against the impact surface. The remaining material overhangs the cask body and is not backed up. Backed up regions project vertically from the target footprint to the cask body, while unbacked regions do not project vertically to the cask. The effectiveness of the energy absorbing crushable material varies depending on whether it is "backed up" by the cask or is unsupported. Two cases are analyzed to bound impact limiter performance. In one case the non backed up material is assumed to be 80% effective and maximum wood crush strength is used (maximum of the possible range based on specified density). In the other case the non-backed up material is assumed to be only 20% effective and minimum wood strength is used. Evaluating impact limiter performance in this way results in a large range of deceleration values, crush forces and crush depth. This in combination with

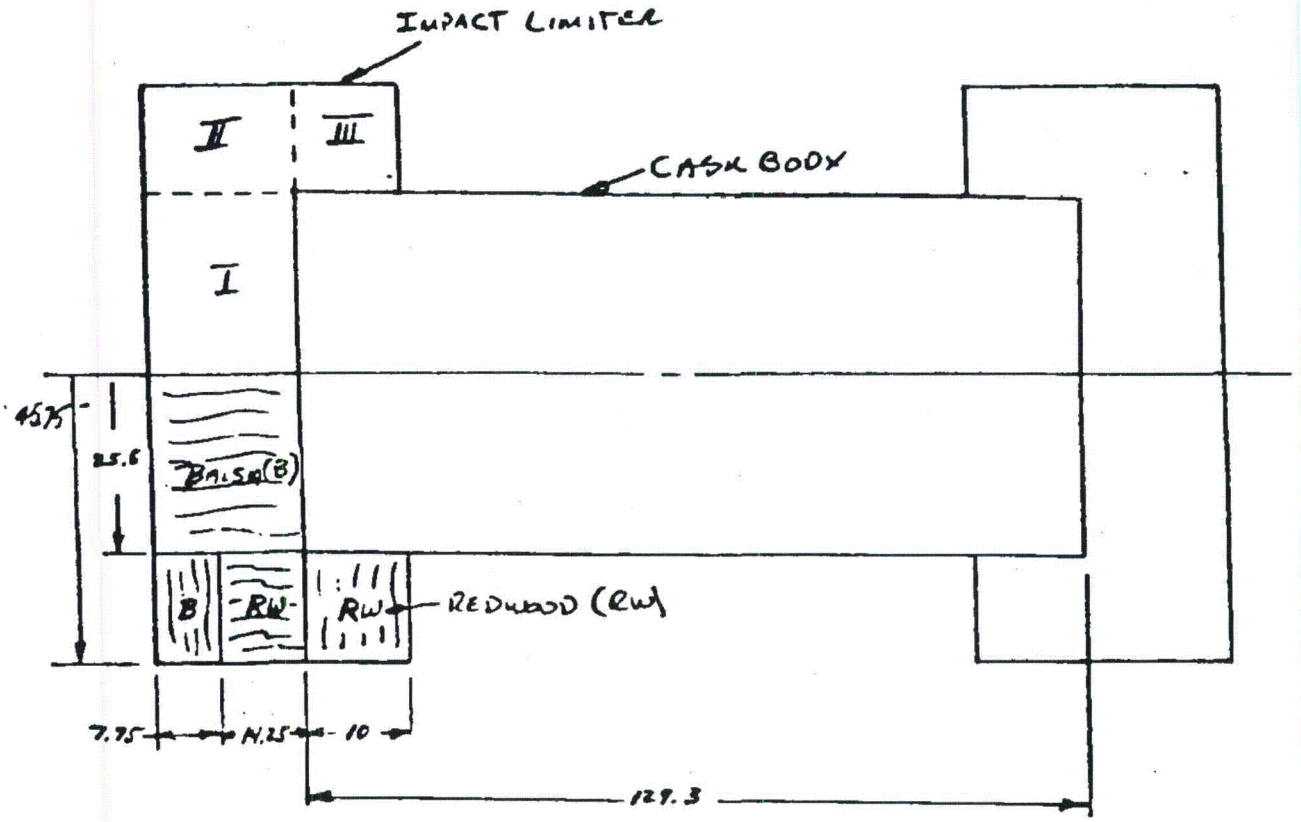

ADOC COMPUTER MODEL FOR TN-RAM PACKAGING

FIGURE 2.10.2-2A

close control of wood properties during procurement assures that the effects of wood properties variation (including temperature effects) and the effectiveness (or lack of effectiveness) of the non backed-up portions of the limiter are covered.

2.10.2.4.4 Analysis Results Predicted by ADOC

The peak inertia loadings or cask body decelerations (in terms of g's) versus initial angle of impact are presented in Tables 2.10.2-3 and 2.10.2-4 for the 30 foot drop. The depth of crush versus initial angle of impact is shown in Tables 2.10.2-5 and 2.10.2-6. Since the packaging CG is within a few inches of the center and the impact limiters are identical, these tables are valid for impact on either end.

In order to determine the cask stresses, these maximum g loads are converted to forces and applied as quasistatic loadings on the outer cask body. A detailed ANSYS finite element model of the TN-RAM cask is used to perform this analysis. Cask body stress analyses are performed for end, side and CG over corner (70°) impact orientations. The lid bolts are analyzed for the maximum axial g load of 80.9 which occurs at an angle of 85°. The full details of the stress analyses are presented in Section 2.10.1.

Based on the crush depths for the side drop from Tables 2.10.2-5 and 2.10.2-6, the trunnions would not hit the target. For the maximum wood properties and 80% effectiveness of non backed-up wood the clearance after the limiters crush would be approximately be 3 1/2 inches. For the minimum wood properties and 20% effectiveness of

TABLE 2.10.2-2

TYPICAL WOOD MATERIAL PROPERTIES

PROPERTY	BALSA	REDWOOD
Density	10-12 lb/ft^3	18.7-27.5 lb/ft^3
Parallel to Grain		
Crush Stress	1560-2010 psi	5000-6500 psi
Locking Strain	0.8	0.6
Unloading Modulus	32,000 psi	1,247,000 psi
Locking Modulus	3,400 psi	4,100 psi
Perpendicular to Grain		
Crush Stress	300-420 psi	750-975 psi
Locking Strain	0.8	0.6
Unloading Modulus	32,000 psi	1,247,000 psi
Locking Modulus	3,400 psi	4,100 psi

TABLE 2.10.2-3

MAXIMUM INERTIA G LOAD VERSUS INITIAL ANGLE OF IMPACT

FOR 30 FEET DROP

MAXIMUM WOOD CRUSH STRESS

EFFECTIVENESS OF NON-BACKED UP WOOD: 80%

	MAXIMUM G LOAD DURING FIRST IMPACT			
		TRANSVERSE		
Initial Angle Of Impact	Axial @ C.G.	Primary Impact End	@ C.G.	Opposite End
90°	69.6	0	0	0
85°	80.9	- 8.5	- 5.0	- 1.5
80°	77.2	-11.8	- 7.47	- 3.18
70°	61.1	-19.4	-13.9	- 8.48
60°	64.7	-31.9	-23.4	-15.0
50°	61.4	-64.0	-35.1	- 6.14
40°	42.1	-67.6	-37.4	- 7.12
30°	34.1	-87.4	-42.4	2.49*
20°	19.7	-86.6	-37.2	12.3 *
10°	13.6	-99.4	-38.5	22.4 *
5°	10.2	-106	-39.2	28.1 *
0°	0	-82.7	-82.7	-82.7
	MAXIMUM G LOAD DURING SECOND IMPACT			
30°	- 4.8	33.5	-34.4	-102
20°	- .23	45.3	-41.1	-128
10°	- .33	49.5	-45.3	-140**
5°	- 0.7	48.9	-45.3	-139

* MAXIMUM ACCELERATION OCCURRED DURING SECOND IMPACT

** MAXIMUM IMPACT FORCE 3,707,000 LB. AT DISTANCE OF 61.14 IN. FROM C.G.

TABLE 2.10.2-4

MAXIMUM INERTIA G LOAD VERSUS INITIAL ANGLE OF IMPACT

FOR 30 FEET DROP

MINIMUM WOOD CRUSH STRESS

EFFECTIVENESS OF NON-BACKED UP WOOD: 20%

Initial Angle Of Impact	MAXIMUM G LOAD DURING FIRST IMPACT			
	Axial @ C.G.	TRANSVERSE		
		Primary Impact End	@ C.G.	Opposite End
90°	47.5	0	0	0
85°	45.3	- 4.7	- 2.32	0
80°	49.6	- 7.89	- 5.51	- 3.12
70°	60.1	-19.4	-14.3	- 9.15
60°	70.4	-35.4	-27.2	-19.0
50°	48.2	-50.7	-27.6	- 4.57
40°	40.4	-76.2	-37.0	2.17
30°	35.4	-106	-46.1	14.2
20°	25.3	-119	-46.9	25.7
10°	7.96	-67.1	-25.2	16.7 *
5°	6.53	-63.6	-23.6	16.4 *
0°	0	-52.7	-52.7	-52.7
	MAXIMUM G LOAD DURING SECOND IMPACT			
10°	-1.36	42.4	-40.3	-123
5°	-0.64	38.0	-36.3	-111

* MAXIMUM ACCELERATION OCCURRED DURING SECOND IMPACT

TABLE 2.10.2-5

DEPTH OF CRUSH VERSUS INITIAL ANGLE OF IMPACT

MAXIMUM WOOD CRUSH STRESS/EFFECTIVENESS OF NON BACKED-UP WOOD: 80%

INITIAL ANGLE OF IMPACT	MAXIMUM CRUSH DEPTH, IN.
90°	6.01
70° (CG Over Corner)	20.5
0°	9.12

TABLE 2.10.2-6

DEPTH OF CRUSH VERSUS INITIAL ANGLE OF IMPACT

MINIMUM WOOD CRUSH STRESS/EFFECTIVENESS OF NON BACKED-UP WOOD: 20%

INITIAL ANGLE OF IMPACT	MAXIMUM CRUSH DEPTH, IN.
90°	9.05
70° (CG Over Corner)	23.8
0°	12.48

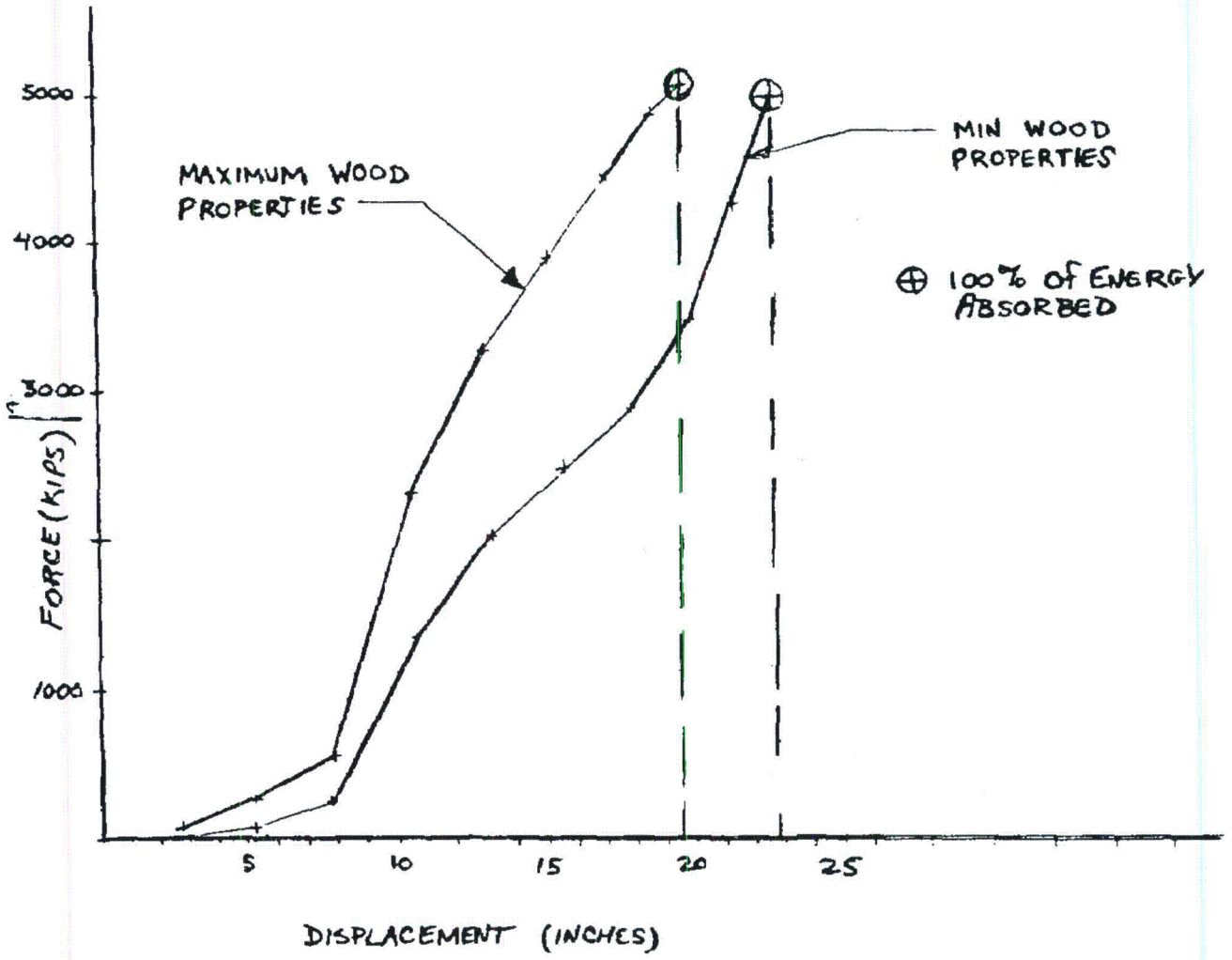

FIGURE 2.10.2-1C

FORCE-DEFLECTION CURVE- CRUSH ON CORNER THRU CASK CENTER OF GRAVITY

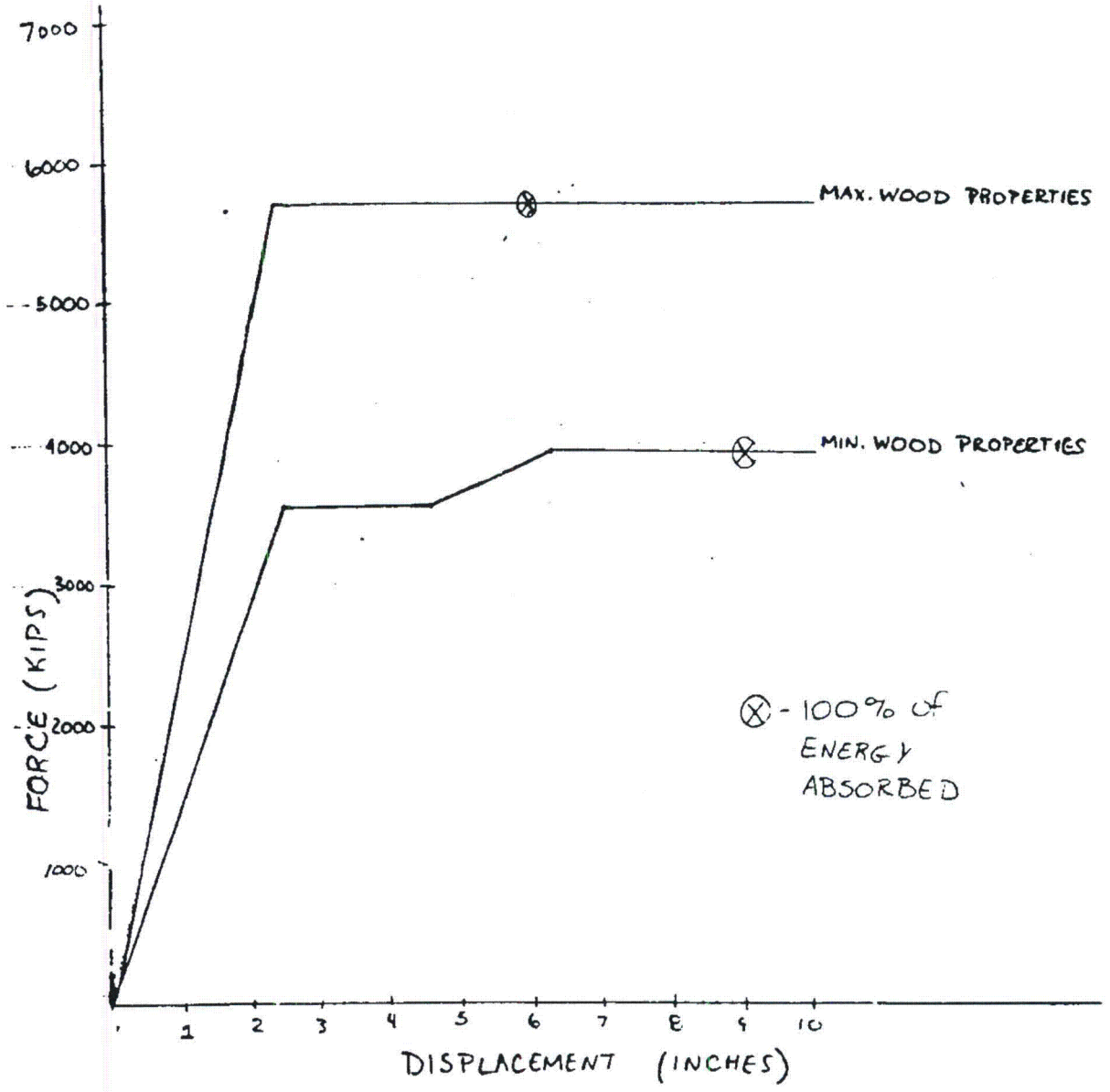

FIGURE 2.10.2-1D
FORCE DEFLECTION CURVE END CRUSH (90°)

FIGURE 2.10.2-1E

FORCE-DEFLECTION CURVE SIDE CRUSH (0°)

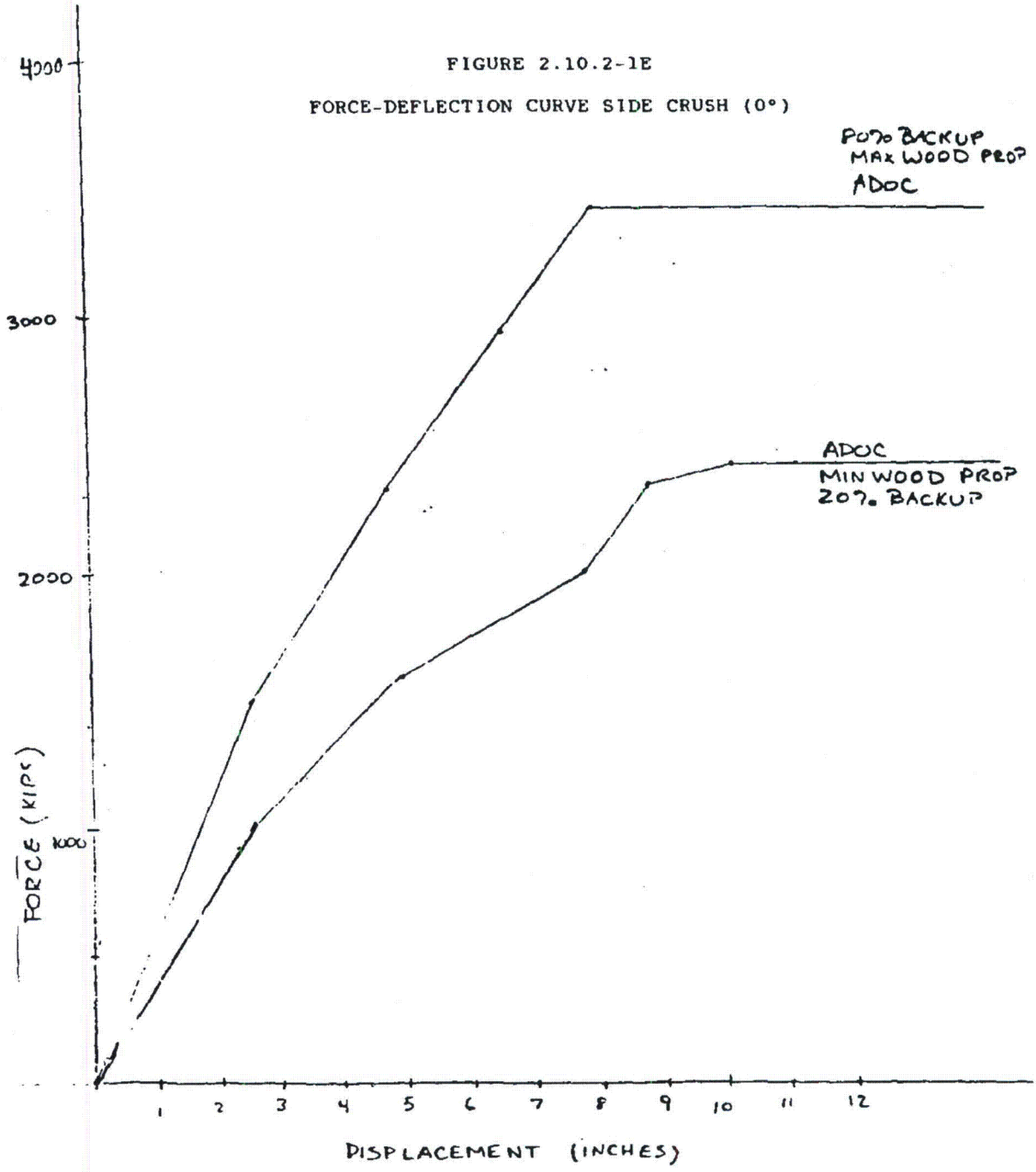

non backed-up wood, the clearance after the limiter crush would be slighly less than 1/2 inch. It is expected that the crush depth would be somewhere between the two bounding cases.

2.10.2.4.5 Results Based on Hand Calculations

The deceleration and crush depths for the end and side drop angles evaluated can be determined by relatively simple hand calculations. These hand calculations were performed and the results are shown below.

End Drop

The deceleration value can be determined by the expression:

$$F = \frac{w\ a}{g}$$

Where

F = crush force, lbs.
w = weight of cask
a = deceleration value
g = acceleration constant

Also

$$F = \sigma_c\ A$$

Where

σ_c = crush stress, psi
A = crush area, in^2

Therefore

$$\frac{a}{g} = \frac{\sigma_c A}{W}$$

The crush stresses of concern for an end drop are those for the balsa.

For the central region (see Figure 2.10.2-2)

$$\sigma_c = 1,560\text{-}2010 \text{ psi}$$
$$A = \pi(25.5^2) = 2,042 \text{ in}^2$$

For the outer region (see Figure 2.10.2-2)

$$\sigma_c = 300\text{-}420 \text{ psi}$$

$$A = \pi(45.75^2 - 25.5^2)\, k$$
$$= 4,533 \text{ in}^2$$

Where

K_{20} = .20 for non backed portion being 20% effective

And

K_{80} = 0.80 for non backed portion being 80% effective

Therefore

$$A_{20} = 4,533 \times 0.2 = 906 \text{ in}^2$$
$$A_{80} = 4,533 \times 0.8 = 3,626 \text{ in}^2$$

The deceleration values are for minimum wood properties:

$$A_{20} = \frac{1,560 \times 2,042 + 300 \times 906}{80,000}$$

$$= 43.2 \text{ g (ADOC Value = 47.5 g)}$$

For maximum wood properties

$$A_{80} = \frac{2,010 \times 2,042 + 420 \times 3,626}{80,000}$$

$$= 70.3 \text{ g (ADOC Value = 69.6 g)}$$

The maximum crush depths can be determined as follows:

$$F \Delta = W \times h$$

Since

$$F = \frac{W a}{g}$$

$$\Delta = \frac{h}{a/g}$$

Therefore for the two bounding cases

$$\Delta_{20} = 360/43.2$$
$$= 8.33 \text{ in (ADOC Value = 9.05 in.)}$$

And

$$\Delta_{80} = 360/70.3$$
$$= 5.12 \text{ in. (ADOC Value = 6.01 in)}$$

As can be seen, the deceleration values calculated by hand agree well with the values predicted by ADOC. The crush depths predicted by ADOC are conservatively higher.

Side Drop

The force crush depth and foot print as each of the limiters crush is shown in Figure 2.10.2-2B. The force (d_f) acting on an element $Rd\theta$ is

$$d_f = \sigma_c B R_o \cos\theta d\theta$$

The energy absorbed as this element deforms is

$$d_E = d_f [A-R_o(1-\cos\theta)]$$
$$= \sigma_c (R_o)^2 B \cos\theta[\cos\theta-\cos\theta]d\theta$$

The total energy absorbed in each of the limiters is obtained by integrating the above.

$$E = 2\sigma_c (R_o)^2 B \int_0^{\theta_o} \cos\theta[\cos\theta-\cos\theta_o]d\theta$$

$$= \sigma_c (R_o)^2 B(\theta_o - \frac{\sin 2\theta_o}{2})$$

The total force in each of the limiters is

$$F = 2\sigma_c B R_o \sin\theta_o$$

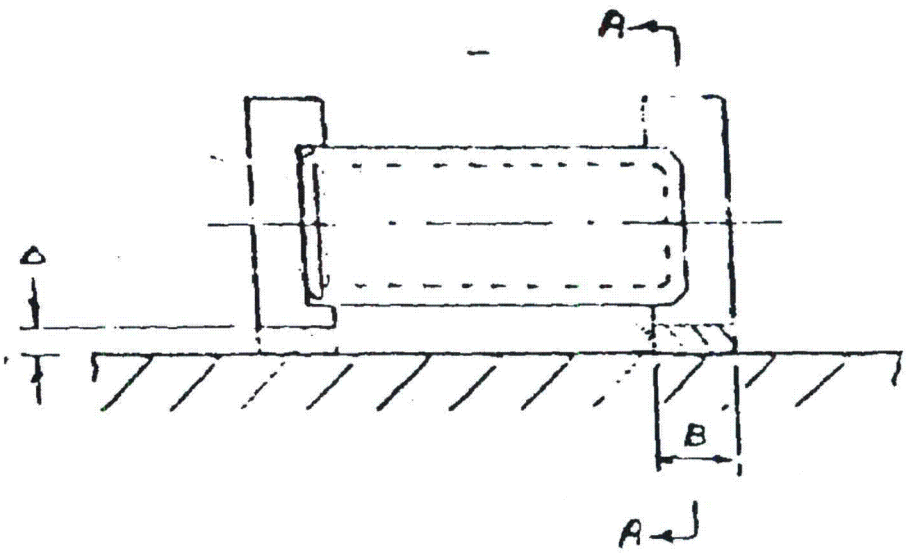

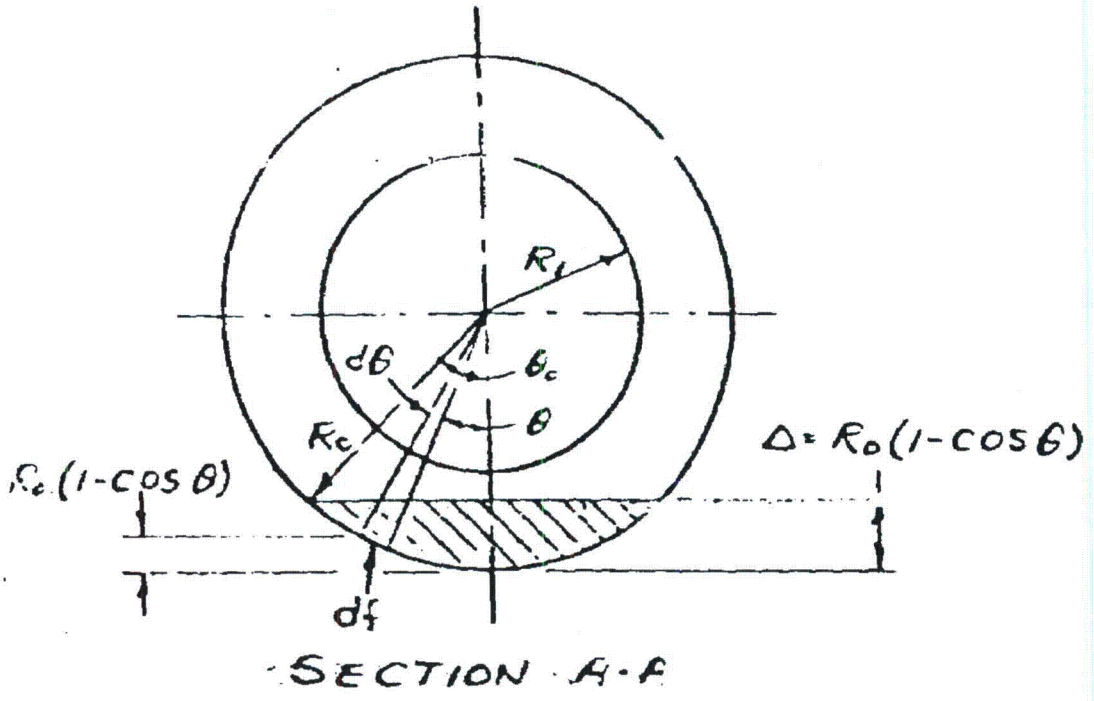

SECTION A-A

CRUSHING OF IMPACT LIMITER FOR SIDE DROP PROBLEM

FIGURE 2.10.2-28

A horizontal drop case is evaluated using the following parameters:

R_o = outside radius of limiters, 45.75 in.
R_i = inside radius of limiter, 25.5 in.
σ_c = average of crush stress, 3,140 psi
B = length of limiter on side which crushes, 24.25 in.
W = 80,000 lb.
H = 360 in.

The total energy to be absorbed is

$$WH = 80,000 \times 360$$

This must be equal to the energy absorbed by deformation of each of the two covers.

$$WH = 2\theta_o(R_o)^2B(\theta_o - \frac{\sin 2\theta_o}{2})$$

$$80,000 \times 360 = 2(3,140)(45.75^2 \times 24.25)(\theta_o - \frac{\sin 2\theta_o}{2})$$

The solution indicates that

θ_o = 30 degrees, $F = 2\sigma_c BR_o \sin 30$
$= 3,482,500$ lbs.

Therefore

$\delta = R_o(1-\cos\theta_o)$
$= 45.75(1-\cos 30)$
$= 6.13$ in.

The peak deceleration, g, is

$$a = \frac{\sigma_c A}{W} = 2(3,140 \times 24.25 \times 45.75 \sin 30)/80,000$$

$$= 87.1 \text{ g}$$

This problem solved with ADOC program gives the following results:

$\theta_o = 36.8°$
$\delta = 9.12$ in.
$a = 82.3$
$F = 3,350,000$ lb.

Again, there is good agreement between ADOC and the hand calculation. It should be noted that the g values and forces used in the analysis for the cask body for the side drop are much higher than predicted by hand calculation or ADOC.

2.10.2.5 SUMMARY DESCRIPTION OF ADOC COMPUTER CODE

One of the critical loadings which must be considered in the design of transport packagings to be used for the shipment or radioactive material is a free drop from thirty-foot height onto an unyielding surface (10CFR71). The packaging must be dropped at an orientation that results in the most severe damage. Impact limiters are usually provided on the packaging to cushion the effects of such impact on the containment portion of the packaging. The limiters are usually hollow cylindrical cups which encase each end of the containment and are filled with an energy absorbing material such as wood or foam.

A computer code, ADOC (Acceleration due to Drop On Covers), has been written to determine the response of a packaging during impact. The analysis upon which this code is based in discussed in this section. The overall analysis of the packaging response is discussed in Section 2.10.2.5.1, and the methods used to compute the forces in the limiters as they crush are presented in Section 2.10.2.5.2.

2.10.2.5.1 General Formulation

The general formulation used to compute the response of the packaging as it impacts with a rigid target is discussed in this section. The assumptions upon which the analysis is based are first presented followed by a detailed development of the equations of motion used to calculate the packaging dynamic behavior. This is followed by a discussion of the numerical methods and the computer code used to implement the analysis. A significant part of the

development is concerned with the prediction of forces developed in the impact limiters as the impact occurs. This aspect of the problem is discussed in Section 2.10.2.5.2.

ASSUMPTIONS

The cask body is assumed to be rigid and axisymmetric. Therefore, all of the energy absorption therefore occurs in the impact limiters which are also assumed to have an axisymmetric geometry. Several assumptions are made in calculating the forces which develop in the limiters as they crush. These are discussed in Section 2.10.2.5.2. Since the packaging is axisymmetric, its motion during impact will be planar. The vertical, horizontal, and rotational components of the motion of the packaging center of gravity (CG) are used to describe this planar motion.

EQUATIONS OF MOTION

A sketch of the packaging at the moment of impact is shown on Figure 2.10.2-3. The packaging is dropped from a height (H), measured from the lowest point on the packaging to the target. The packaging is oriented during the drop, and at impact, so that the centerline is at an angle (θ) with respect to the horizontal. At the instant of impact, the packaging has a vertical velocity of:

$$V_0 = \sqrt{2gH} \qquad (1)$$

Where,

g = gravitational constant

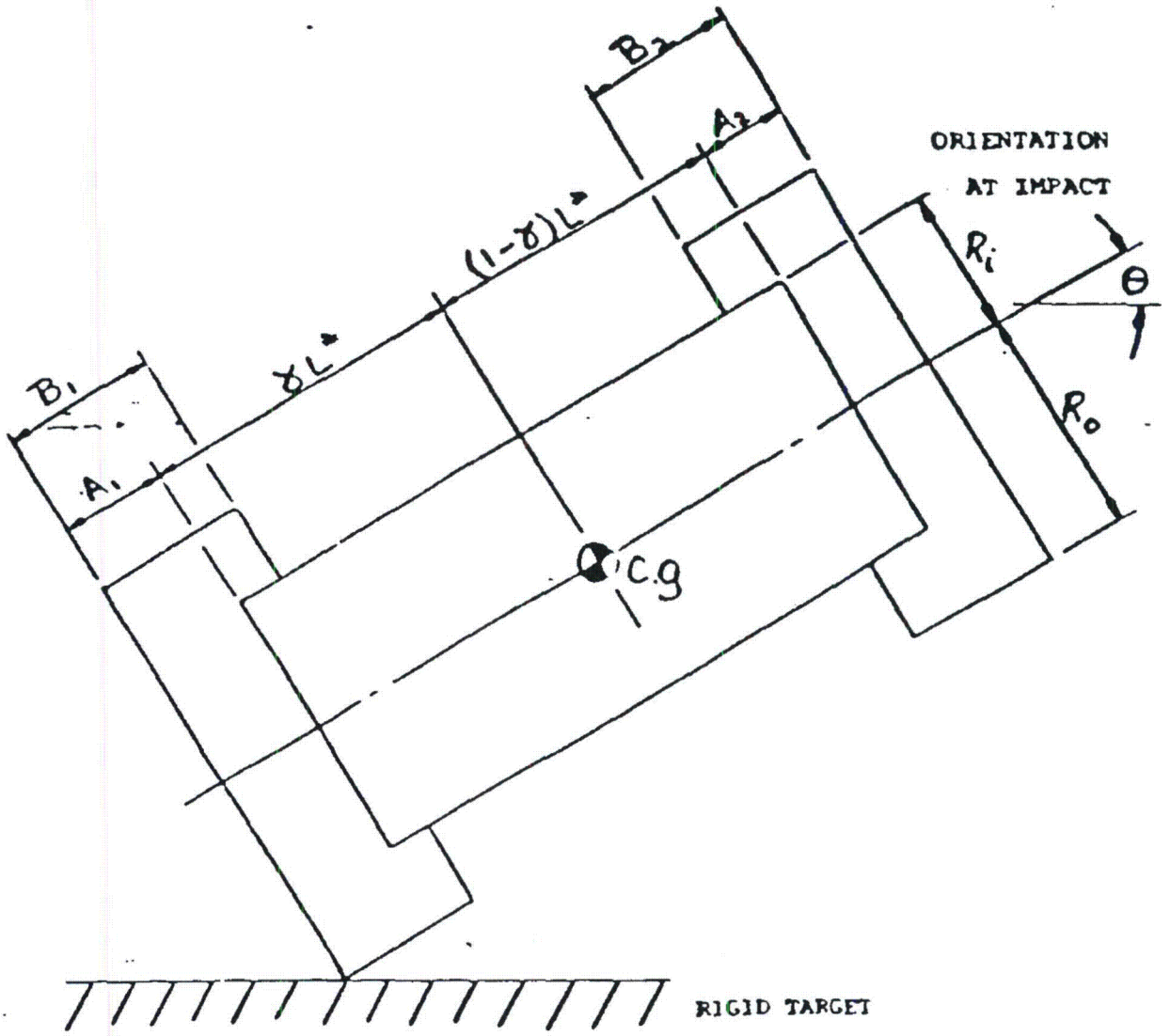

GEOMETRY OF PACKAGING

FIGURE 2.10.2-3

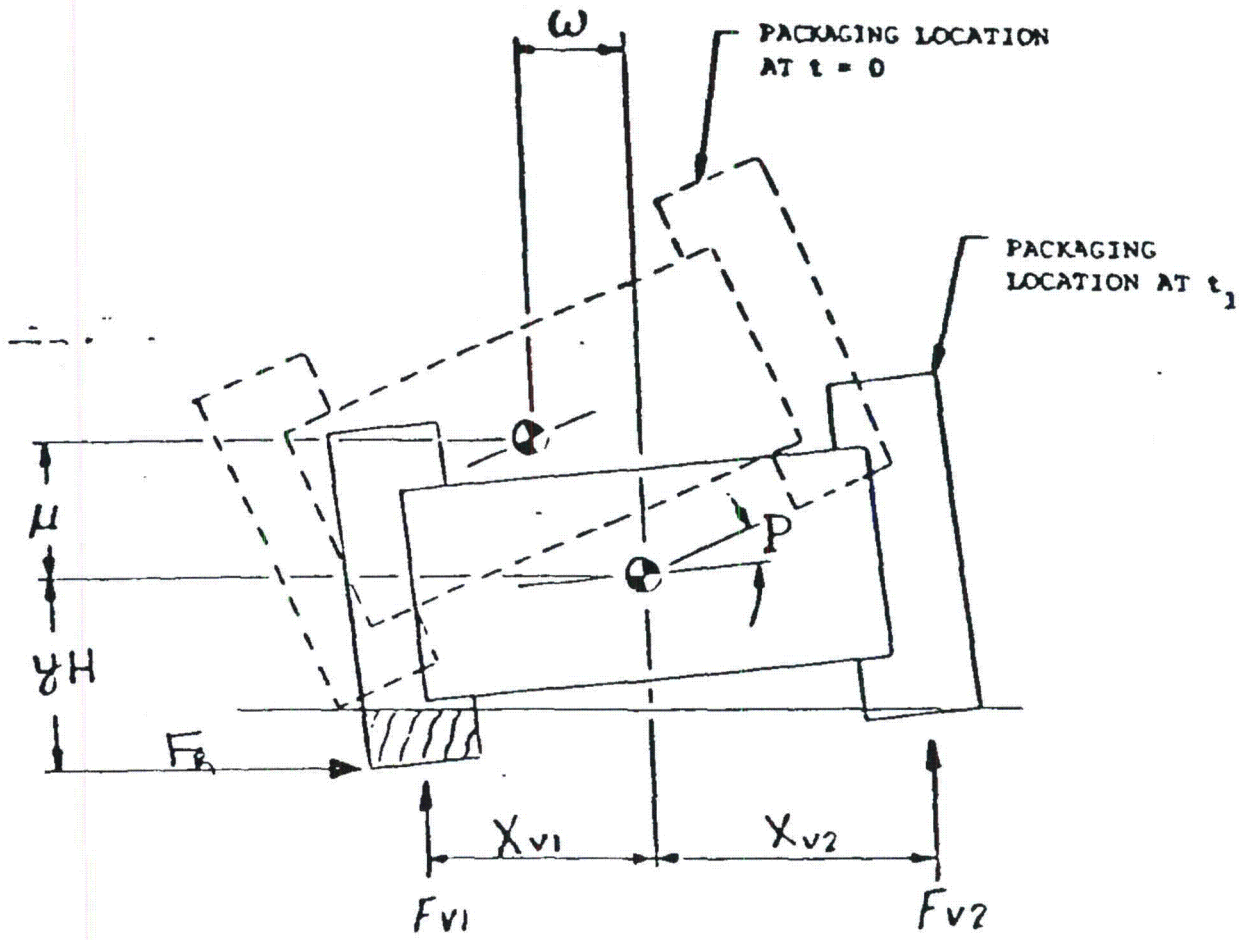

PACKAGING LOCATION AT TIME (t)

FIGURE 2.10.2-4

At some time (t) after first impact, the packaging has undergone vertical (u), horizontal (w), and rotational (ρ) displacements. The location of the packaging at this time is shown on Figure 2.10.2-4. One or both of the limiters have been crushed as shown. The resulting deformations (and strains) in the limiters result in forces which the limiters exert on the packaging, thereby decelerating it. These forces, and their points of application on the packaging, are shown on Figure 2.10.2-4 as F_{v1}, F_{v2} and F_h. The method used to calculate these forces and the points of application is given in Section 2.10.2.5.2, below.

The three equations of motion describing the motion of the cask are:

$$M\ddot{u} + F_{v1} + F_{v2} - W = 0 \qquad (2)$$

$$M\ddot{w} - F_h = 0 \qquad (3)$$

$$J\ddot{\rho} - F_{v1} X_{v1} + F_{v2} X_{v2} + F_h Y_h = 0 \qquad (4)$$

Where,

M = mass of packaging

J = polar moment of inertia of the packaging about its CG

$(\ddot{})$ = acceleration

At impact (t = 0), all of the initial conditions are zero except that $u' = V_0$.

COMPUTER SOLUTION

The computer code is written to compute the motion of the packaging during impact. The solution is obtained by numerically integrating the equations of motion (equations 2, 3, and 4) from the time of impact (t = 0) to a specified maximum time (t_{max}). The integrations are carried forward in time at a specified time increment (Δt). Parametric studies indicate that a time increment of 1 msec is sufficiently small so that further reduction of the time increment does not affect the results. Solutions are usually carried out to about 150 msec for the near horizontal drops and to about 50 msec for the near vertical drops. The significant motions of the packaging normally occur within these time periods.

A standard fourth order Runge Kutta numerical integration method is used to perform the numerical integrations. The following procedure is used to carry the solution from time (t_i) to time (t_{i+1}). Note that at time (t_i) the displacements and velocities of the three degrees of freedom describing the motion of the CG of the packaging are known.

(1) Calculate the deformation of each of the limiters based on the packaging geometry and the motion of the packaging's CG (see Section 2.10.2.5.2 for details).

(2) Calculate the forces which the limiters exert on the packaging body using the deformation of the limiters and their stress-strain characteristics (see Section 2.10.2.5.2 for details).

(3) Use Equations 2, 3, and 4 to calculate the accelerations during the time interval.

(4) Use the Runge Kutta equations to calculate the location and velocity of the cask CG at time (t_{i+1}).

(5) Go to step (1) to repeat the process until time = t_{max}.

(6) Generate the output.

Output from the code consists of:

Problem title, packaging geometry, drop conditions, and integration data.

Limiter geometric and material property data.

History of packaging CG motion and amount of crushing in each of the limiters.

Force history data.

Plot of acceleration histories.

Plot of maximum limiter deformations.

2.10.2.5.2 Forces in Limiters

The methods used to calculate the forces (F_{v1}, F_{v2}, and F_h) in the limiter caused by a given crush depth are discussed in this

section. These calculations are used to perform steps (1) and (2) above. The limiter geometry and material specification is discussed first. The general methodology used to calculate the forces are then presented which is followed with a detailed development of the equations used to calculate the force-displacement relationships.

LIMITER GEOMETRY

A sketch of the model of a limiter is shown on Figure 2.10.2-5. Regions I, II and III are used to delineate regions where different materials are used. It should be noted that the properties of the three regions are designed to accommodate the crush requirements of the three significant drop orientations. The properties of regions I, II and III are selected to control the decelerations resulting from vertical, corner, and shallow drop orientations, respectively. The properties used to describe the stress-strain behavior of each of the three materials are discussed below. The dimensions (A) and (B) may vary for the limiters at each end of the packaging, but (R_o) and (R_i) are taken to be the same for both limiters. The same material properties are used for each of the limiters.

GENERAL APPROACH

The ideal energy absorbing material is one that has a stress-strain curve that has a large strain region where the stress is constant. Such a materials absorbs the maximum energy while minimizing force (which determines the magnitude of the deceleration). Wood, foam, and honeycomb materials exhibit such behavior and are prime candidates for impact limiter crushable material. If the constant

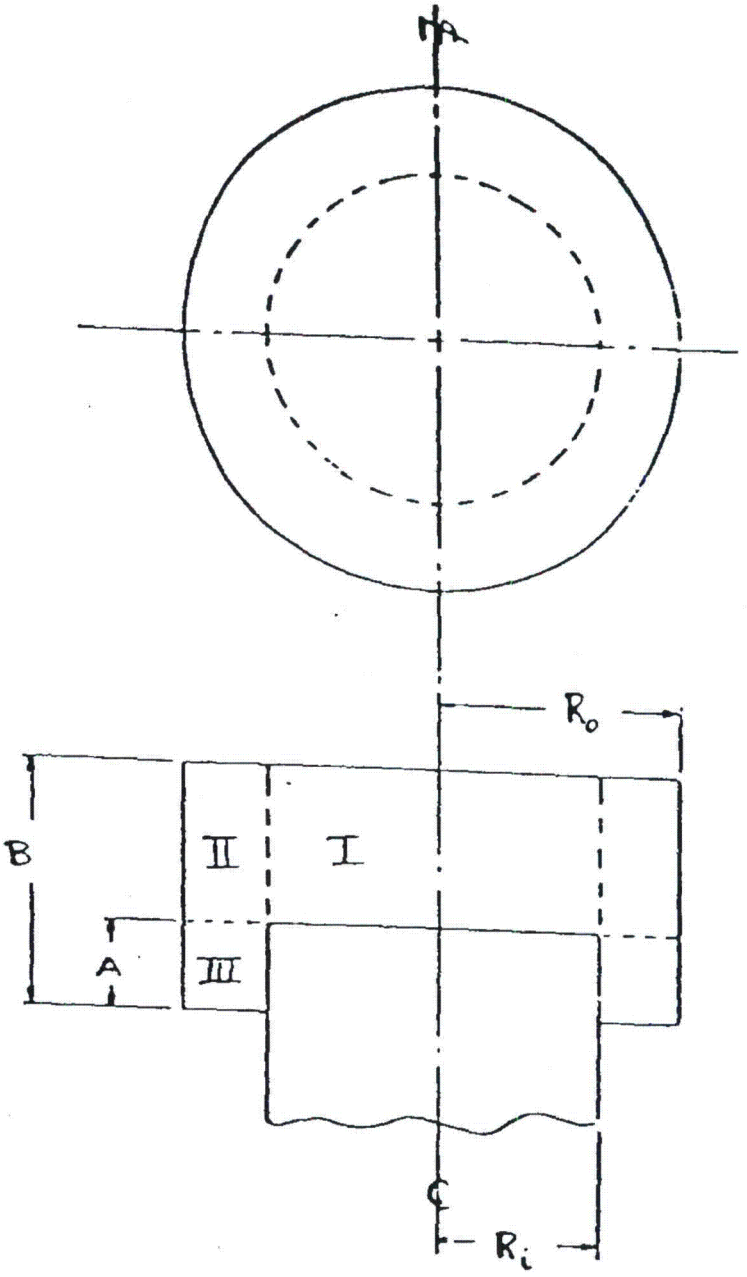

GEOMETRY OF LIMITER

FIGURE 2.10.2-5

stress region of the stress-strain curve is of primary interest, the forces may be calculated as the crush stress times the area of the surface defined by the intersection of the target with the doughnut shape of the impact limiter. This approach assumes that the crush stress, which acts normal to the crush surface, is not influenced by stresses acting in directions parallel to the crush surface (i.e., the confining stresses). This assumption is made in the computer code. The crush stress used as input to the code is selected to represent that value which is consistent with the degree of confinement afforded by the impact limiter geometry for the drop orientation considered. Therefore, the crushable material is modeled in the code with a one dimensional (oriented normal to the crush surface) stress-strain law. The properties of the stress-strain law are selected to represent the degree of confinement provided by stresses acting in the other two dimensions. The properties of the crushable material are not modified as the packaging rotates but are selected to represent the material properties for the initial crush direction of the material.

A portion of the "crushed" area of the limiter is often not backed up by the packaging body (i.e., a projection of a point in this non backed up area normal to the target (impact surface) does not intersect the cask body). The user must specify the percentage of these forces which are to be included in the calculation. The confinement provided by the overall construction of the limiter will determine the extent to which these non backed up forces are actually effective:

It should be emphasized that the computer code does not perform any computations which would allow the user to judge the adequacy of the selected percentage of non backed-up forces which are counted.

The evaluation of the impact area and its centroid (required to locate the impact forces) is computationally complicated because of the many variations possible in the manner in which the target intersects the limiter. This problem is resolved by dividing the surface of the limiter into many small segments. The segment is located relative to the target at each computation. If the segment's original location is below the target, then it has crushed and it contributes a force equal to the stress times its area projected on the target. The location of this force is also known. The strain at the segment may also be evaluated so that the peak strains may be determined and stresses may be evaluated for strains which fall outside of the constant crush stress region of the stress-strain law.

The forces must be calculated at each time that the solution for the packaging response is computed. The problem, therefore, is to determine the forces acting on the limiters given the current location of the packaging center of gravity. The solution for the location of the packaging center of gravity is discussed in Section 2.10.2.5-1. The procedure used to perform these computations is as follows (each of the steps is detailed below).

(1) Define the location of the target relative to the limiters from the current location of the packaging center of gravity relative to the target.

(2) Divide the surface of the limiter into segments and calculate the strain in a one dimensional element spanning the distance between the center of the segment and the packaging body.

(3) Compute the stress in the element from the stress-strain relationship. Multiply the stress by the area of the element projected onto the target.

(4) After all of the segments on the limiter are evaluated, sum the segment forces and moments of the forces to find the total force and moment acting on the packaging.

(5) Calculate the horizontal force and moment of the horizontal force.

(6) Use equations 2, 3, and 4 to extend the solution to the next time step. The new solution consists of the location of the packaging CG at the new time. The above steps are then repeated. This process is continued until the specified maximum time is reached.

DETAILS OF FORCE COMPUTATIONS

Details of each of the six steps outlined above are given in this section. Note that the location of the packaging CG is known at the beginning of this computational sequence.

Deformation of the Limiter

The first step in the computation is to evaluate the location of the limiters relative to the target given the location of the packaging CG relative to the target. The limiter position relative to the target is defined by the six variables (D_1 through D_6) as shown

on Figure 2.10.2-6. The location of the cask at first contact is shown on Figure 2.10.2-6a with the subscript (o) added to the D's indicating initial values. The initial values of these parameters (when the lowest corner of the packaging first contacts) are found from geometric considerations:

$$
\begin{aligned}
D_{10} &= 2R_0 \cos\theta \\
D_{20} &= 0 \\
D_{30} &= B_1 \sin\theta \\
D_{40} &= D_{30} + D_{10} + L^* \sin\theta + B_2 \sin\theta \\
D_{50} &= D_{40} - D_{10} \\
D_{60} &= D_{30} + L^* \sin\theta
\end{aligned}
\qquad (5)
$$

At a given time (t) the packaging CG has displaced vertically (u), horizontally (w), and has rotated (ρ) and reached the position shown in Figure 2.10.2-6b. Each of the six points have then fallen by an amount:

$$\Delta D = u*l(\sin\theta - \sin(\theta-\rho)) + r(\cos\theta - \cos(\theta-\rho)) \qquad (6)$$

Where,

l = axial distance CG to point (+CG to top)

r = radial distance CG to point (+CG to impact)

Then the corner deformations become:

$$D_i = D_i - \Delta D_i$$

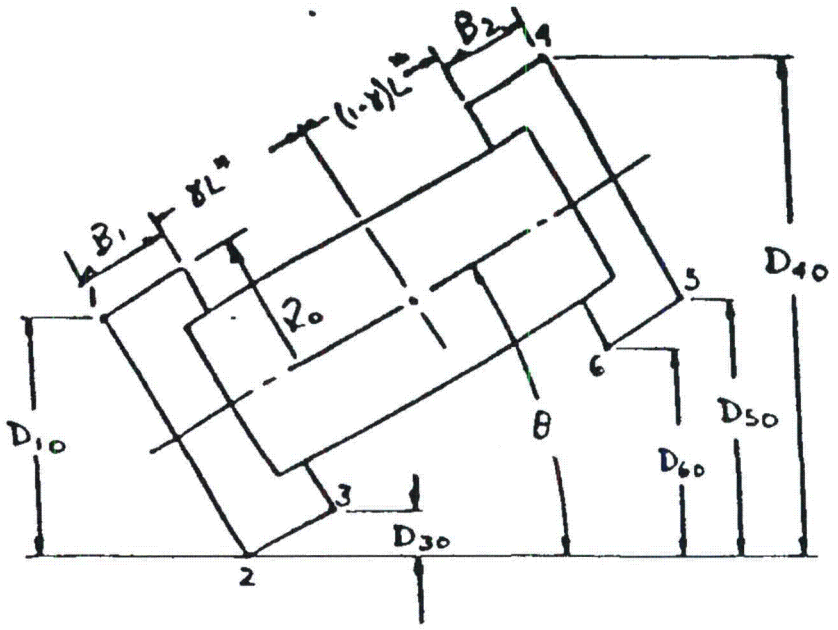

a. Impact Limiter Parameters at First Impact

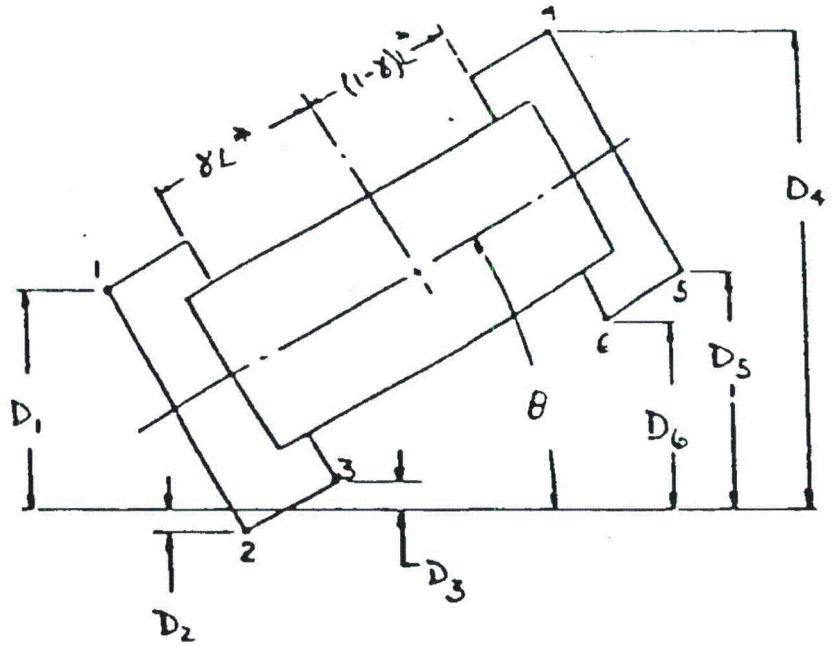

b. Impact Limiter Parameters - General

DEFINITION OF LIMITER DEFORMATION

FIGURE 2.10.2-6

Where,

$$l_1 = l_2 = -yL^* - B_1$$
$$l_3 = -yL^*$$
$$l_4 = l_5 = (1-y)L^* + B_2$$
$$l_6 = (1-y)L^*$$
$$r_1 = r_4 = -R_0$$
$$r_2 = r_3 = r_5 = r_6 = R_0$$

To facilitate the computation of strains in the limiter, the position of the limiter relative to the impact surface is classified as shown in Figure 2.10.2-7. There are three possible locations of the impact surface relative to the limiter. The task is therefore to define which of the three patterns apply, and to determine the parameters (ϕ) and (Δ) in terms of the variables D_1 through D_6, just determined.

These deformations are next related to the three types of crush patterns for the bottom limiter shown on Figure 2.10.2-7. Crush pattern I applies when:

$$D_1 < 0;\ D_2 < 0;\ D_3 > 0 \qquad (8)$$

Then,

$$\Delta = -D_2/\cos\phi \qquad (9)$$

$$\phi = \cos^{-1}\left((D_3-D_2)/B_1\right)$$

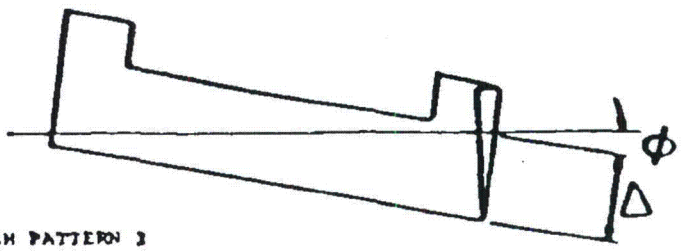

a. CRUSH PATTERN I

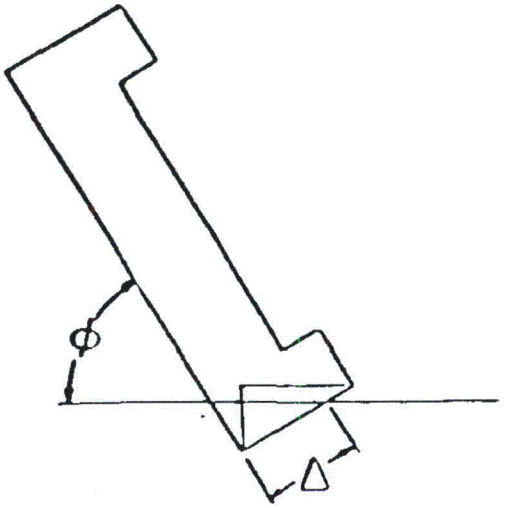

b. CRUSH PATTERN II

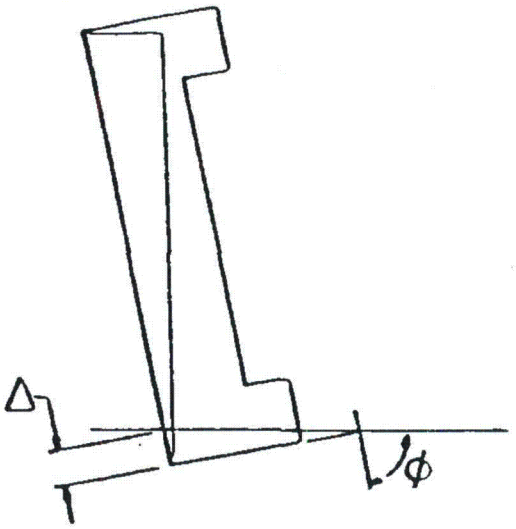

c. CRUSH PATTERN III

CRUSH PATTERN IN LIMITER

FIGURE 2.10.2-7

Crush pattern II applies when:

$$D_1 > 0;\ D_2 < 0;\ D_3 > 0 \qquad (10)$$

Then,

$$\Delta = -D_2/\cos\phi \qquad (11)$$

$$\phi = \cos^{-1}((D_3-D_2)/B_1)$$

Crush pattern III applies when:

$$D_1 > 0;\ D_2 < 0;\ D_3 < 0 \qquad (12)$$

Then,

$$\Delta = D_2/\sin\phi \qquad (13)$$

$$\phi = \sin^{-1}((D_1-D_2)/2R_0)$$

The same set of equations apply to the top limiter if (D_1, D_2, D_3, B_1) are replaced with (D_4, D_5, D_6, B_2) in equations (8) through (13).

Strains in Limiters

The next step in the computation is to calculate strains in the limiters given the deformation defined above. The limiters are first divided into segments as shown in Figure 2.10.2-8. The number of segments used for the bottom (NB) and the sides (NS) are input by the user. Locations on the surface of the limiters are described in terms of the (R,Z,β) coordinate systems shown on the figure. Strains in the segments along the sides of the limiters are calculated based on the location of the center of the segment (R_0,Z,β). The segments at the bottom are divided into two pieces: one for $R < R_i$ (i.e. in Region 1) and the second for R

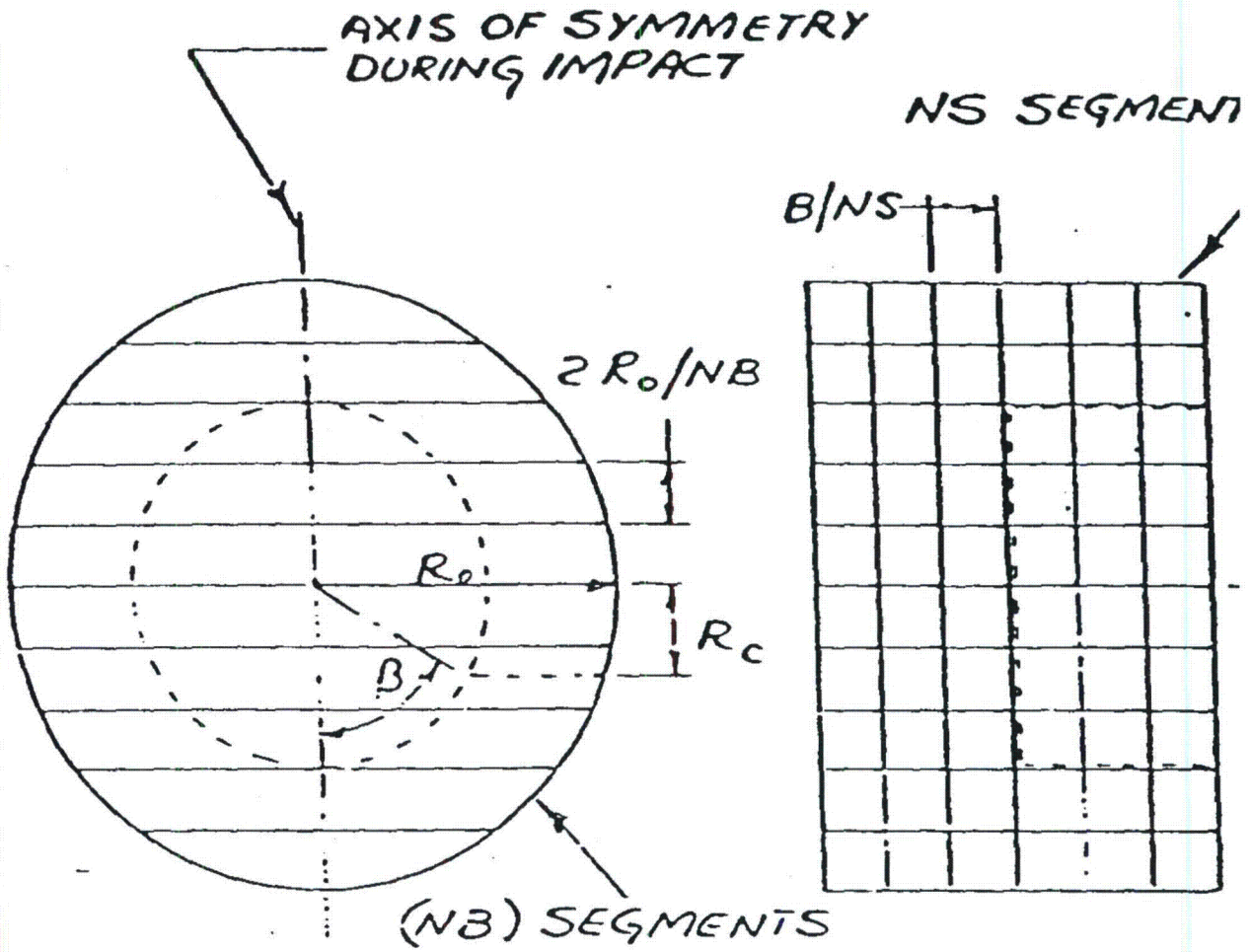

SEGMENTED LIMITER

FIGURE 2.10.2-8

$> R_i$. A strain is calculated for each of these two pieces for each segment along the bottom surface.

The strains (ε) are calculated as the deformation of the point normal to the crush surface (δ) divided by the undeformed distance of the point from the surface of the limiter to the outer container (q), again measured normal to the crush surface. Therefore:

$$\varepsilon = \delta/q \qquad (14)$$

Different equations govern each of these parameters for each of the three crush patterns as shown on Figure 2.10.2-7.

The geometry for crush pattern I is shown on Figure 2.10.2-9. Forces resulting from deformation of the side elements are neglected for this crush pattern. It may be shown that the deformation is:

$$\delta = \Delta \cos \phi + (R \cos \beta - R_0) \sin \phi \qquad (15)$$

The undeformed length of the element is taken measured to the plane of the packaging bottom so that:

$$q = A_1 \cos \phi \qquad (16)$$

The geometry for crush pattern II is shown on Figure 2.10.2-10. The deformation of the points on the bottom (a) and along the side (b) may be represented with the same equation:

$$\delta = \Delta \cos \phi + (r \cos \beta - R_0) \sin \phi - Z/\cos \phi \qquad (17)$$

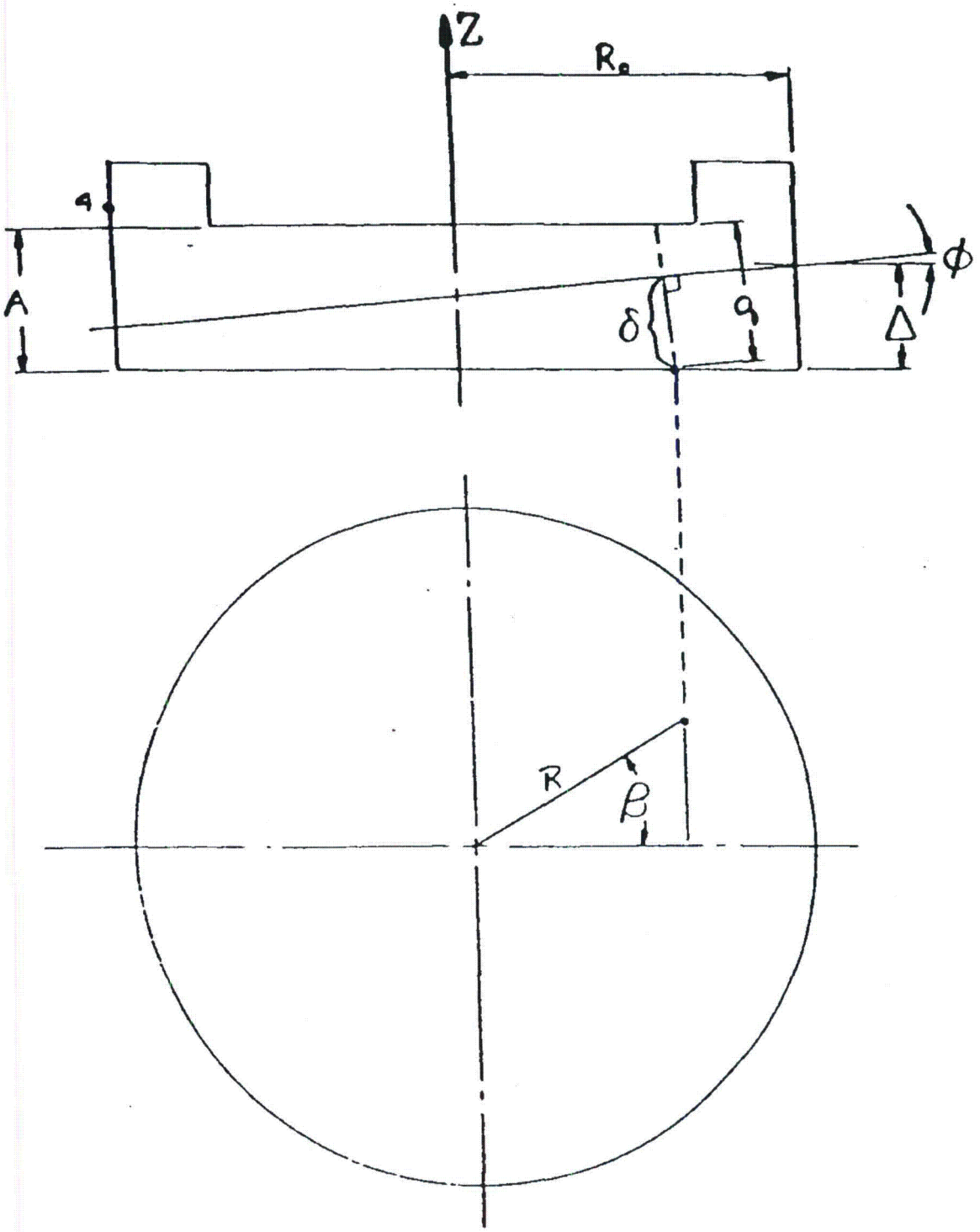

STRAIN COMPUTATION FOR CRUSH PATTERN 1

FIGURE 2.10.2-9

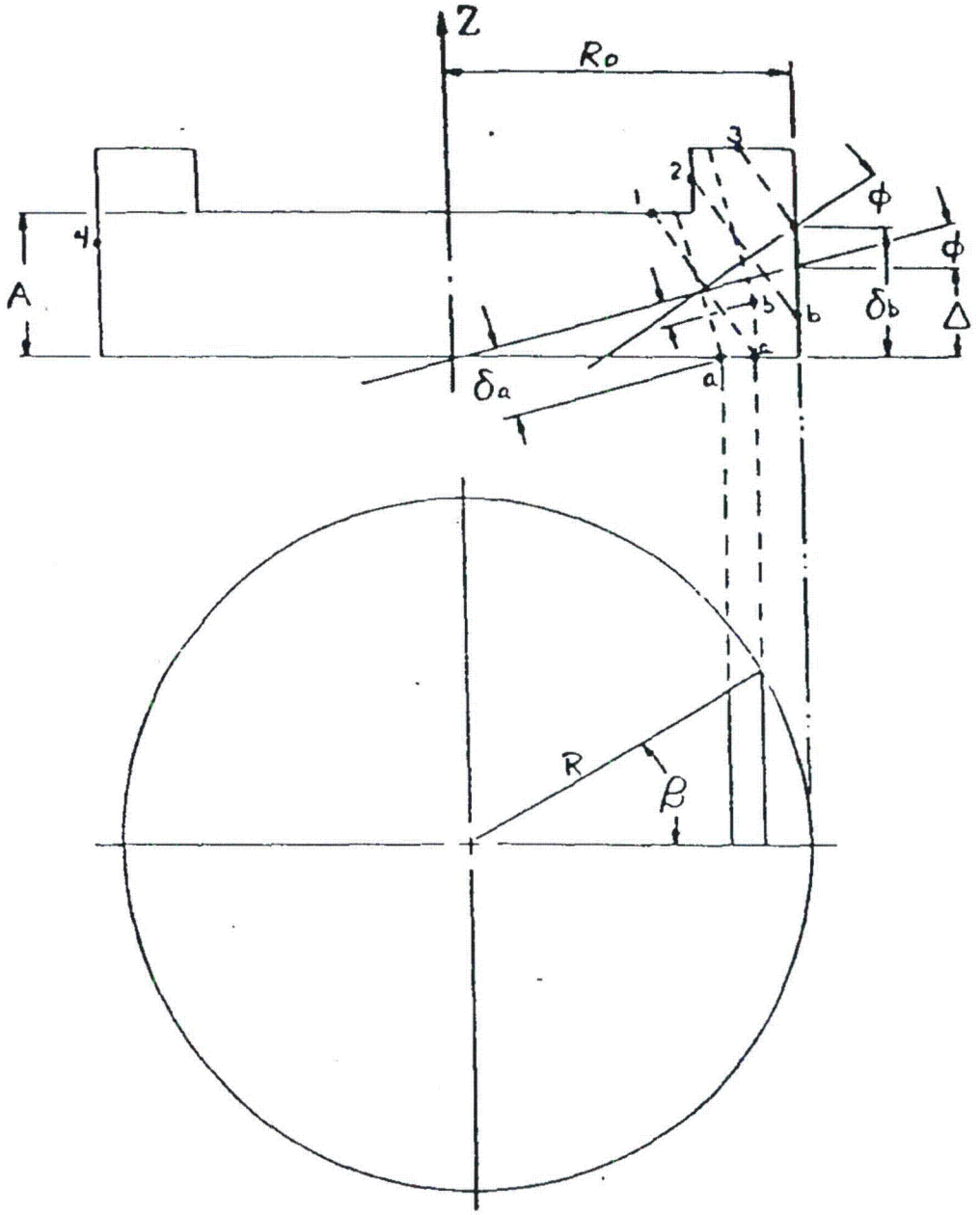

STRAIN COMPUTATION FOR CRUSH PATTERN II

FIGURE 2.10.2-10

The original length of the element depends on the intersection of the projection of the point on the impact surface with the outline of the limiter. Four points are identified as shown on Figure 2.10.2-10. The lengths are:

$$\begin{aligned} q_1 &= (A-Z)/\cos\phi \\ q_2 &= X/\sin\phi \\ q_3 &= (B-Z)/\cos\phi \\ q_4 &= ((R_0^2 - R^2\sin^2\beta)^{1/2} + R\cos\beta)\sin\phi \end{aligned} \qquad (18)$$

Where,

$$X = R\cos\beta + (R^2\cos^2\beta - R_2 + R_1^2)^{1/2}$$

The deformation for crush pattern III is shown on Figure 2.10.2-11. Deformations of points on the bottom of the limiter are neglected for this crush pattern. The deformation is:

$$\delta = (\Delta - Z/\tan\phi - R_0(1 - \cos\beta))/\sin\phi$$

The original length is measured to (R_i) so that:

$$q = (R_0 - R_i)/\sin\phi \qquad (20)$$

Segment Stress

The stresses in the elements are calculated from the above strains. As mentioned above, three sets of stress-strain laws are input to the code, one for each of the regions defined in Figure 2.10.2-5.

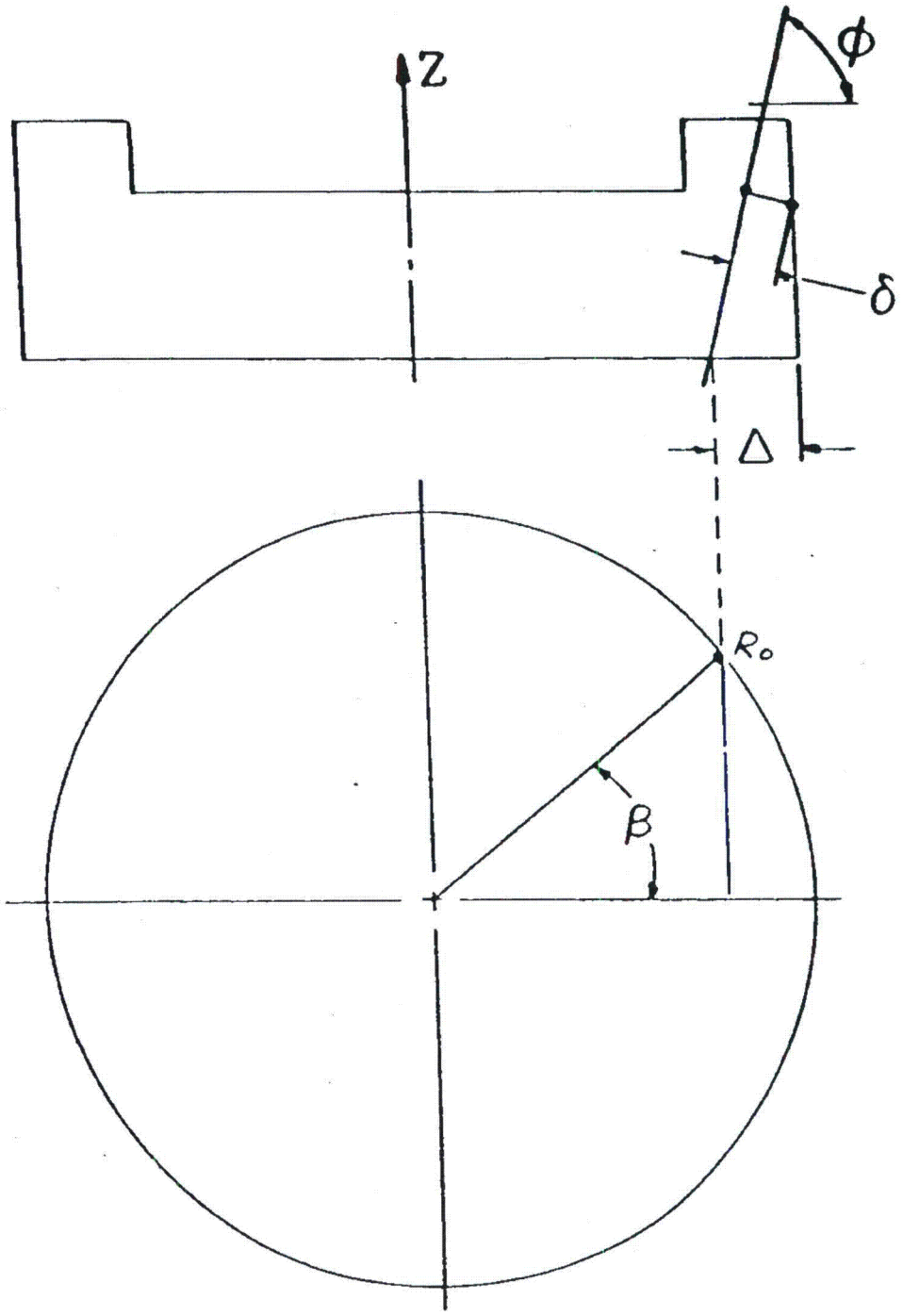

STRAIN COMPUTATION FOR CRUSH PATTERN III

FIGURE 2.10.2-11

The location of the center of the segment on the surface of the limiter is used to determine which of the three stress-strain laws is to be used. The model may be viewed as a set of one dimensional rods which run from the center of the segment, normal to the target, to another boundary of the limiter. The entire rod is given the properties which the limiter material has at the beginning point of the rod (i.e., the intersection with the target).

The stress-strain law used for the materials is shown on Figure 2.10.2-12. Each of the seven parameters shown on the figure is input to the code for each of the three regions of the limiter. The arrows on the figure indicate the load-unload paths used in the model. The step in the crush strength is built into the stress-strain law so that two crushable materials in series may be modeled. The two crush strengths should be specified as the actual crush strengths of the two materials. The first locking strain (ϵ_1) should be specified as the locking strain of the weaker material times the length of the weaker material divided by the total specimen length. The higher locking strain (ϵ_L) should be specified as the first locking strain plus the locking strain of the stronger material times its length and divided by the specimen length.

As stated above, the properties of the limiter material are not varied as the limiter crushes and the packaging rotates. Limiter materials such as wood exhibit anisotropic material properties. This must be accounted for when the properties are input to the code based on the anticipated direction of crushing. Most of the anisotropic wood data is based on tests performed in the elastic

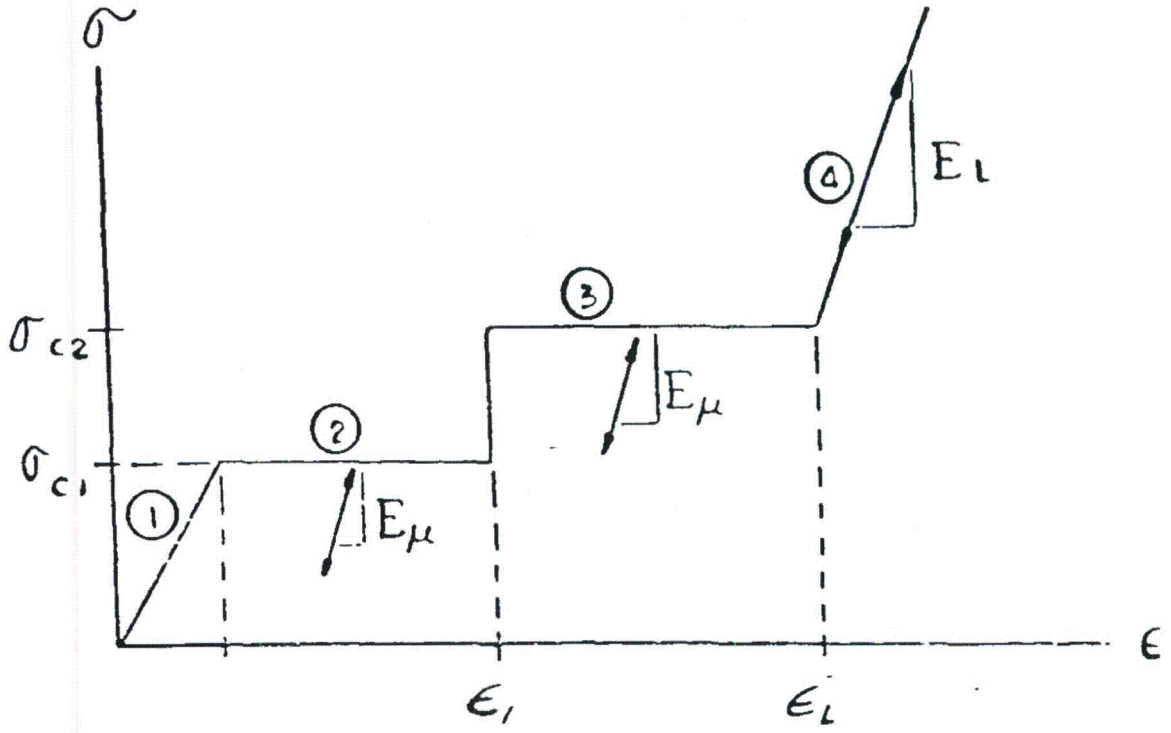

WOOD STRESS - STRAIN CURVE

FIGURE 2.10.2-12

range. The following relationship has been used to represent wood properties for a loading which is applied at an angle (α) with respect to the wood grain:

$$P = (P_1 COS^4 \alpha + P_2 SIN^4 \alpha)(/COS^4 \alpha + SIN^4 \alpha) \quad (21)$$

Where,

P = property of interest

P_1, P_2 = properties parallel and perpendicular to grain

Evaluation of Forces

The stresses determined above are multiplied by the area of the segment projected onto the crush surface. The areas of the sidewall segments are (see Figure 2.10.2-8):

$$A_s = 2R_O \, B \, COS(\theta - \rho)/(NB \, NS \, TAN \, \beta) \quad (22)$$

The area of the bottom segments is divided into two parts, one in region I and the other in region II. These areas are:

$$A_b = 4R_O L_b SIN(\theta - \rho)/NB \quad (23)$$

Where,

$$L_b = (R_i^{\,2} - R_c^{\,2})^{1/2}; \text{ region I}$$

$$= (R_O^{\,2} - R_c^{\,2})^{1/2} - (R_i^{\,2} - R_c^{\,2})^{1/2}; \text{ region II}$$

These forces are summed for all of the elements to determine the total force acting on the packaging. The forces are also multiplied by their moment arms about the packaging CG to calculate the total moment acting on the packaging. The point on the segment is first projected, normal to the target, to evaluate whether or not it intersects the packaging body. If the projection does not intersect the packaging body, only a percentage of the force is included in the summation. The user specifies the percentage to be used.

Horizontal Force

A horizontal force develops at the limiter/target interface. This force is only considered for the bottom limiter (i.e., the first to impact) since the packaging is always close to horizontal when the top impact limiter is in contact.

The horizontal force (F_h) is first calculated as that required to restrain horizontal motion of the tip of the limiter.

The horizontal acceleration ($\ddot{\Delta}_H$) at the tip of the bottom limiter (point 2 on Figure 2.10.2-6) may be related to the CG motion of the packaging by:

$$\ddot{\Delta}_H = \ddot{w} - \ddot{\rho}[(\gamma L^* + B_1) \cos \phi + R_0 \sin \phi] \qquad (24)$$

Where,

$$\phi = \pi/2 - \theta + \rho$$

Equating $\ddot{\Delta}_H$ to zero would result in no acceleration of the tip in the horizontal direction and provides the solution of w in terms of ρ.

Substituting this solution for w into Equation (3) results in an expression for the horizontal force (F_h), required to restrict horizontal acceleration of the tip, in terms of the rotational acceleration (ρ). Finally, equation 4 is used to eliminate (ρ) with the result,

$$F_h = M_v W[\gamma L^* + B_1)\cos\phi + R_0 \sin\phi]/ J_g + W[(\gamma L^* + B_1)\cos\phi + R_0 \sin\phi]^2 \quad (25)$$

Where,

M_v = moment due to vertical forces = $F_{v1}x_{v1} - F_{v2}x_{v2}$
W = packaging weight

This force is restricted to:

$$F_h < \mu F_{v1} \quad (26)$$

Where,

μ = coefficent of friction specified by user

2.10.2.6 ANALYSIS FOR ONE FOOT DROP NORMAL CONDITION

This section describes the analysis of the TN-RAM for the one foot normal drop condition. The TN-RAM is lifted vertically and is transported horizontally. End and side drop orientations are therefore considered to be credible normal drop events. Any other drop orientation will cause the cask to tip over onto its side, clearly an accident. The accident analyses in Section 2.10.2.4 bound any possible tipping accident. Therefore, the one foot drop analysis is performed only for the end and side drop orientations.

The packaging kinetic energy is again assumed to be absorbed by crushing of the impact limiters. The dynamic system model of Section 2.10.2.4 was used to perform the side drop (0°) analysis using the ADOC computer program described in Section 2.10.2.5. The end drop analysis was performed assuming that the energy would be absorbed by the soft balsa wood (oriented in the weak direction) in the outer end of the limiter. This is a very accurate way to determine g loads on an end drop since the g values can be calculated by the expression F = Ma where F = crush stress times the area and M = package weight divided by the acceleration of gravity g.

The inertial load results of these one foot drop analyses are presented in Table 2.10.2-7. Again, two extreme cases are considered. The upper bound stiffness case assumes maximum wood crush strength and 80% effectiveness of non backed-up wood. The lower stiffness case assumes minimum wood strength and only 20% effectiveness of non backed-up wood. The actual case will be between these upper and lower bounds. Stress analyses in Section 2.10.1 are performed for the case(s) with maximum inertia loads.

TABLE 2.10.2-7

MAXIMUM INERTIAL G LOAD DURING ONE FOOT DROP

	INITIAL ANGLE OF IMPACT	MAXIMUM G LOAD AXIAL (ALL LOCATIONS)	MAXIMUM G LOAD TRANSVERSE (ALL LOCATIONS)
MAXIMUM WOOD CRUSH STRESS AND 80% EFFECTIVENESS OF NON-BACKED UP WOOD	90° (End Drop)	29.8	0
	0° (Side Drop)	0	-36.3
MINIMUM WOOD CRUSH STRESS AND 20% EFFECTIVENESS OF NON-BACKED UP WOOD	90° (End Drop)	21.27	0
	0° (Side Drop)	0	-24.4

2.10.2.7 IMPACT LIMITER ATTACHMENT ANALYSIS

The impact limiter attachments are designed to keep the impact limiters attached to the cask body during all normal and hypothetical accident conditions. The loading which has the highest potential for detaching the impact limiter is the slapdown or secondary impact after a shallow angle 30 foot drop. During this impact, the crushing force on the portion of the impact limiter beyond the cask body (the non backed-up area) tends to pull the limiter away from the cask. The end and corner drops are not critical cases for the impact limiter attachments since the impact force tends to push the impact limiter onto the cask in these orientations.

For the attachment bolt analysis, maximum effectiveness of the non-backed up wood and maximum wood crush strengths of 2010 psi for balsa and 6500 psi for redwood are assumed. The maximum wood properties produce the highest overturning moment on the limiter. Based on the dynamic analysis performed using the ADOC code, the most severe slapdown impact occurs after a shallow angle oblique impact at 10° initial angle. The peak deceleration and contact force at the end of the cask body subjected to secondary impact (slapdown) are maximum for this case. The peak deceleration is 140 g's and the peak force is 3,707,000 lb. as indicated in Table 2.10.2-3.

The maximum moment applied to the impact limiter attachments is conservatively determined ignoring the mass of the impact limiter which tends to reduce the attachment forces. The center of the

external impact force on the limiter is 5.60 in. from the center of the cask reaction force. Therefore, the net moment applied to the limiter by the impact force couple is $3.707 \times 10^6 \times 5.60$ or 20.75×10^6 in. lb. This moment is reacted by the eight impact limiter attachment bolts.

A free body diagram of the impact limiter is shown in Figure 2.10.2-13. It is conservatively assumed that the impact limiter pivots on the edge of the cask end. The maximum force, F, occurs in the bolt farthest from the pivot point, and the bolt force varies linearly with distance from the pivot point.

The moment of inertia of the bolting pattern about the corner of the cask (pivot point) is:

$$I_{xx} = \frac{nr}{2}_o^2 A_b + n A_b \left(\frac{d}{2}\right)^2 = 16,614 \text{ in.}^4$$

Where:

d = cask dia. = 51.25 in.

n = number of bolts = 8

r_o = bolt circle radius = 27.63 in.

A_b = bolt area for $1\frac{3}{4}$ -8 UNC bolts = 2.00 in.^{2}

The distance from the pivot point to the highest stressed (farthest) bolt is 53.25 in. Therefore, the maximum attachment bolt tensile stress is Mc/I or 66,506 psi. This conservatively calculated stress is well below the minimum attachment bolt ultimate tensile strength of 140,000 psi. The factor of safety against bolt failure is 2.10. Therefore, the bolts will not yield and will hold the limiter on the cask.

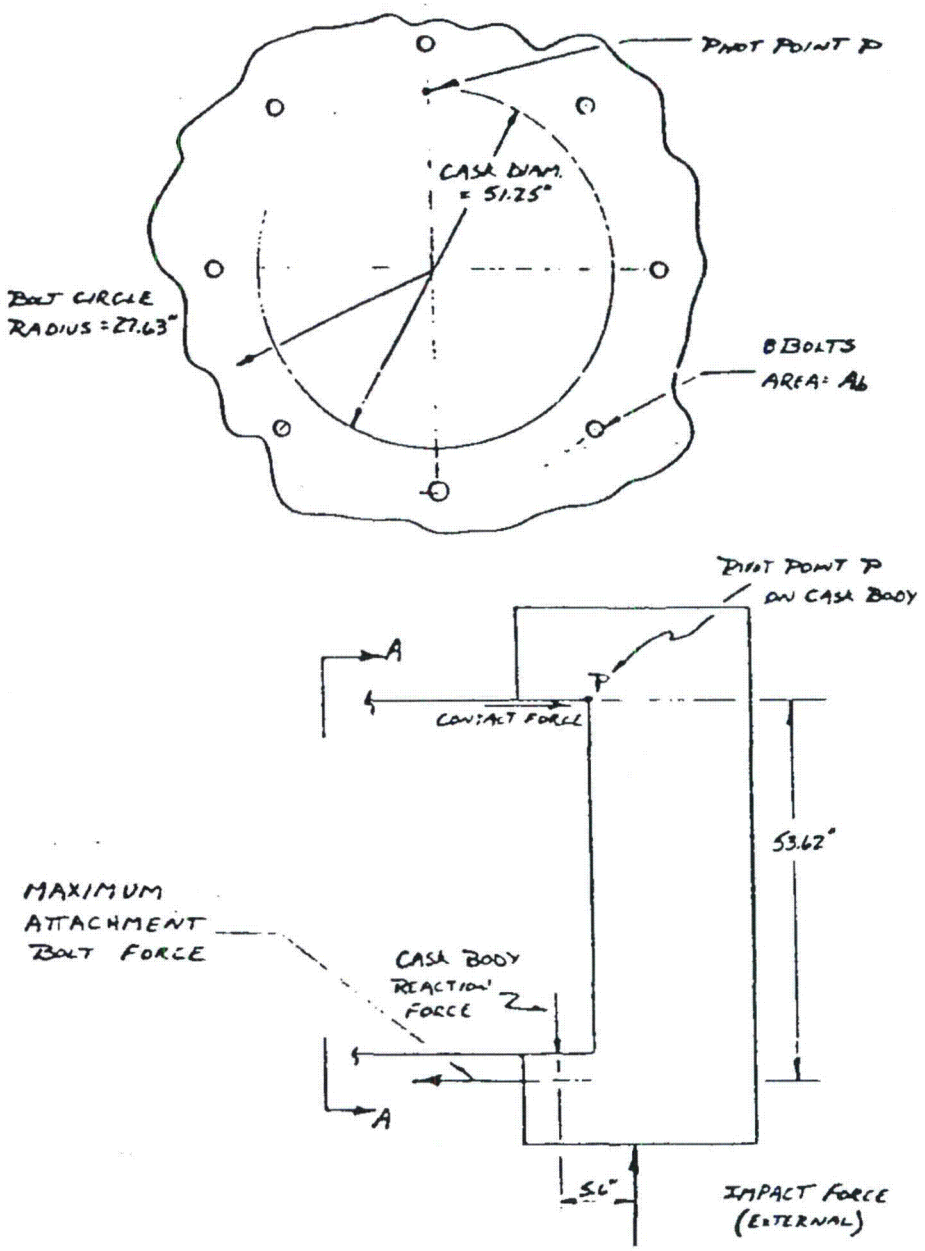

FREE BODY DIAGRAM OF IMPACT LIMITER FOR DETERMINING ATTACHMENT BOLT LOADS

FIGURE 2.10.2-13

2.10.2.8 IMPACT LIMITER PRESSURE ANALYSIS

The impact limiters are designed to be leaktight during normal transport conditions so that the moisture content, and hence crush strength, of the impact limiter materials is maintained. The outer shell of the impact limiter is designed to withstand pressure differences due to elevation and temperature changes during transit. The impact limiters are equipped with fusible disks which melt during the hypothetical thermal accident thus preventing excessive pressure buildup.

This section presents the analysis of the impact limiter structure during normal transport conditions. The impact limiters are sealed at ambient temperature, 68°F, and pressure, 14.7 psia. The maximum temperature of the limiters during normal transport conditions is 120°F. The pressure increase due to this rise in temperature is:

$$\Delta P = P_i \left(\frac{T}{T_i}\right) - P_i$$

$$\Delta P = 14.7 \ \frac{579.7°R}{527.7°R} \ -14.7 = 1.5 \text{ psi}$$

The reduced external pressure due to elevation changes is approximately 3 psi. These pressures are combined resulting in a uniform total pressure of 4.5 psi.

The gussets in the impact limiter are spaced so that the average length of any flat plate section of the outer shell is 18.5 inches.

Assuming the plate edges are fixed and that there is a uniform pressure difference applied on the entire surface, the maximum stress at the center of the plate is:

$$\sigma = \frac{\beta w b^2}{t^2}$$

Roark, RJ, "Formulas for Stress and Strain", Fourth Edition Case 41 pg. 226

where,

b = 18.5 inches
t = 0.125 inches thick
w = uniform load, psi

and β = 0.3078, a function of the plate geometry.

Limiting the maximum outer plate bending stress to 1.5 times the 30,000 psi yield stress results in an allowable uniform load of:

w = 6.67 psi

Therefore, the impact limiter shell is capable of withstanding simultaneous internal and external pressure fluctuations (1.5 psi plus 3 psi) during normal conditions of transport.